Helical Chirality Induction in Zinc Bilindiones by Amino Acid Esters and Amines

Tadashi Mizutani,*[,1] Shigeyuki Yagi,[2] Atsushi Honmaru,[1] Shinji Murakami,[2] Masaru Furusyo,[3] Toru Takagishi,[2] and Hisanobu Ogoshi*[,1,4]

Department of Synthetic Chemistry and Biological Chemistry, Graduate School of Engineering, Kyoto University, Yoshida, Sakyo-ku, Kyoto 606-8501 Japan, Department of Applied Materials Science, Osaka Prefecture University, Gakuen-cho, Sakai, Osaka 599-8531 Japan, CAE Research Center, Sumitomo Electric, Ltd., Hikari-dai 1-7, Seika-cho, Souraku-gun, Kyoto 619-0237 Japan, and Fukui National College of Technology, Geshi, Sabae, Fukui 916-0064 Japan

Received April 30, 1998

Complexation of α-amino acid esters, *β*-amino ethers, and amines with a series of zinc 1,19-bilindione derivatives was studied, particularly focusing on the helical chirality induction in the bilindione framework triggered by the binding of chiral guests. Comparative studies of binding and helical chirality induction indicated that binding and chiral induction were markedly affected by polar substituents present in both zinc bilindiones and guests. 2-Hydroxyethyl groups at the 2,18-positions of zinc bilindione largely assisted the binding of amines and amino acid esters but not the chiral induction. 19O-Alkylation of the zinc bilindiones had inhibitory effects on the binding but enhanced efficiency of helical chirality induction. The enantiomeric excess of 19O-alkyl zinc bilindione complexed with L-Trp-OMe in CD_2Cl_2 was 73% at 223 K. A COOR group and an aromatic group in the guest promoted helical chirality induction of 19O-alkylated zinc bilindiones. The patterns of ^{1}H NMR complexation-induced shifts of zinc bilindiones and guests and a molecular modeling study of the complexes showed that electrostatic repulsion between the COOR group of amino acid esters and the lactam ring of zinc bilindiones, and stacking of the side chain groups of amino acid esters on the C ring of zinc bilindione made a significant contribution to efficient helical chirality induction.

Conformational changes induced by molecular recognition are closely related to the functions of many biological processes as seen in allosteric enzymes, for example. To elucidate the nature of interactions inducing conformational changes in a model system, a flexible host with well-defined conformations[5] is required. The zinc complexes of 1,19-bilindione derivatives (ZnBD) have two degenerate helical conformations with right-handed helicity (*P*-form) and left-handed helicity (*M*-form),[6] which are rapidly interconverting in a solution.[7] By addition of a chiral guest, the conformation of ZnBD can be driven to preferred chirality.[8−11] Helical chirality induction has two important implications. First, helical structures are seen in proteins and DNAs as a structural motif, and their helical sense is ultimately determined by the chirality of constituent monomers. Therefore, the favorable combination of point chirality of a monomer and helical chirality of the resultant polymer should be important for stability of such highly organized biomolecules.[12,13] Second, understanding of the mechanism of helical chirality induction would lead to the utilization of helical molecules as an auxiliary group for asymmetric synthesis[14] or as a chirality probe.[15] The helical chirality induction by a chiral guest having only one chiral carbon attracts interest, since such a system can be a simplest model for helical structure formation from simpler chirality.

For the classification of chirality, point chirality is only one of chemical structural feature, while helical chirality is functional in the sense that it will determine the motional direction, for instance. Understanding the mechanism of point chirality−helical chirality interconversion is thus important from the view of the structure−function relationship. We report here that chiral α-amino

(1) Kyoto University.
(2) Osaka Prefecture University.
(3) Sumitomo Electric, Ltd.
(4) Fukui National College of Technology.
(5) Hoffmann, R. W. *Angew. Chem., Int. Ed. Engl.* **1992**, *31*, 1124−1134.
(6) (a) Bonfiglio, J. V.; Bonnett, R.; Hursthouse, M. B.; Malik, K. M. *J. Chem. Soc., Chem. Commun.* **1977**, 83−84. (b) Balch, A. L.; Mazzanti, M.; Noll, B. C.; Olmstead, N. M. *J. Am. Chem. Soc.* **1994**, *116*, 9114.
(7) Lehner, H.; Riemer, W.; Schaffner, K. *Liebigs Ann. Chem.* **1979**, 1798.
(8) (a) Lightner, D. A.; Gawronski, J. K.; Wijekoon, W. M. D. *J. Am. Chem. Soc.* **1987**, *109*, 6354. (b) Krois, D. *Tetrahedron* **1993**, *49*, 8855−8864.
(9) For chiral induction in biliverdin by complexation with proteins, see: (a) Huber, R.; Schneider, M.; Mayr, I.; Muller, R.; Deutzmann, R.; Suter, F.; Zuber, H.; Falk, H.; Kayser, H. *J. Mol. Biol.* **1987**, *198*, 499−513. (b) Marko, H.; Mueller, N.; Falk, H. *Monatsh. Chem.* **1989**, *120*, 163. (c) Trull, F. R.; Ibars, O.; Lightner, D. A. *Arch. Biochem. Biophys.* **1992**, *298*, 710−14. (d) Wagner, U. G.; Muller, N.; Schmitzberger, W.; Falk, H.; Kratky, C. *J. Mol. Biol.* **1995**, *247*, 326−337.
(10) For biliverdin bearing chiral peptides via a covalent bond, see: (a) Krois, D.; Lehner, H. *J. Chem. Soc., Perkin Trans. 2* **1987**, 219−225. (b) Krois, D.; Lehner, H. *J. Chem. Soc., Perkin Trans. 2* **1987**, 1523−1526. (c) Krois, D.; Lehner, H. *J. Chem. Soc., Perkin Trans 2* **1990**, 1745−1755.
(11) For chirally bridged biliverdins, see: (a) Krois, D.; Lehner, H. *J. Chem. Soc., Perkin Trans. 2* **1989**, 2085−2090. (b) Krois, D.; Lehner, H. *J. Chem. Soc., Perkin Trans. 1* **1989**, 2179−2185. (c) Krois, D.; Lehner, H. *J. Chem. Soc., Perkin Trans. 2* **1993**, 1351−1360. (d) Krois, D.; Lehner, H. *J. Chem. Soc., Perkin Trans. 2.* **1993**, 1837−1840.
(12) Green, M. M.; Peterson, N. C.; Sato, T.; Teramoto, A.; Cook, R.; Lifson, S. *Science* **1995**, *268*, 1860.
(13) For review of supramolecular chemistry of helical molecules, see: Piguet, C.; Bernardinelli, G.; Hopfgartner, G. *Chem. Rev.* **1997**, *97*, 2005−2062.
(14) Reetz, M. T.; Beuttenmüller, E. W.; Goddard, R. *Tetrahedron Lett.* **1997**, *38*, 3211−3214.
(15) Yashima, E.; Matsushima, T.; Okamoto, Y. *J. Am. Chem. Soc.* **1997**, *119*, 6345−6359.

10.1021/jo980819j CCC: $15.00
Published on Web 11/01/1998

Scheme 1

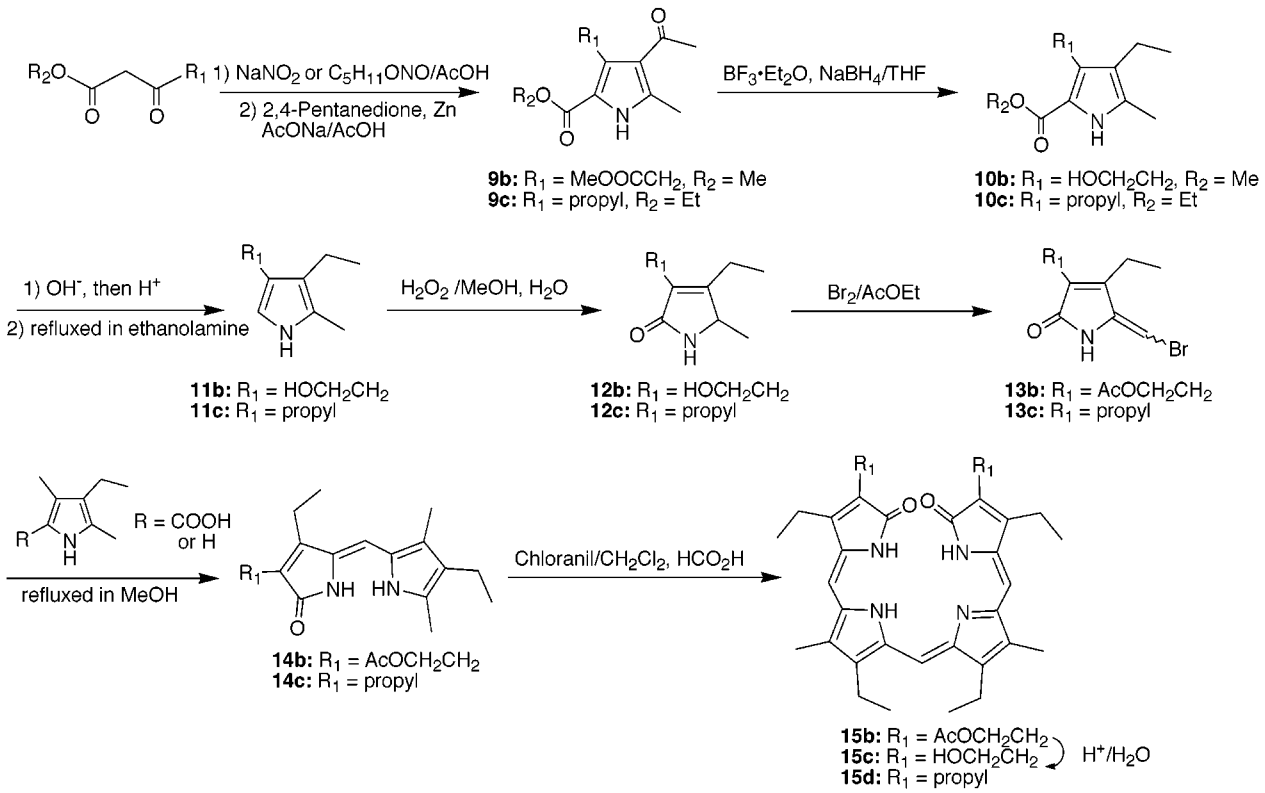

acid esters, *β*-amino ethers, and amines induced helical chirality in a series of ZnBDs upon complexation.[16] Forces that effectively induce chirality were elucidated on the basis of systematic investigations on the complexation equilibria by use of variable-temperature NMR, circular dichroism (CD), and UV−vis spectroscopies and molecular modeling studies.

Results and Discussion

Zinc bilindiones **1**−**8** were prepared according to the Lightner's route (Schemes 1 and 2).[17] Dipyrrole **14** was

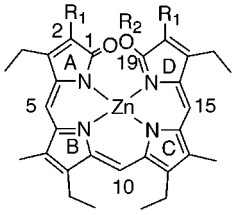

1: $R_1 = CH_3$, $R_2 = H$
2: $R_1 = CH_2CH_2OH$, $R_2 = H$
3: $R_1 = CH_2CH_2OAc$, $R_2 = H$
4: $R_1 = CH_3$, $R_2 = CH_3$
5: $R_1 = CH_2CH_2OH$, $R_2 = CH_3$
6: $R_1 = CH_2CH_2OAc$, $R_2 = CH_3$
7: $R_1 = CH_2CH_2CH_3$, $R_2 = CH_3$
8: $R_1 = CH_3$, $R_2 = CH(CH_3)_2$

prepared from trialkylpyrrole **11**. Coupling of **14b** yielded O-acetylated compound **15b**, which was acid-hydrolyzed to give bilindione **15c**. Other bilindiones, **15a**, **15c**, and **15e**, were similarly prepared. To convert bilindione **15** to 19O-alkyl bilindione **17**, reactions developed by Fuhrhop[18] were employed. Thus, bilindione **15** was reacted with acetic anhydride to afford the oxoniaporphyrin **16**, which was readily cleaved by a nucleophilic attack of alkoxide ions and metalated to yield the zinc complexes of 19O-alkylated bilindiones **4**−**8**. For the preparation of **5** and **6**, 1 equiv of a methoxide ion afforded **6** and excess methoxide afforded **5**. ZnBDs **1**−**8** were characterized by ^{1}H NMR, IR, UV−vis, and high-resolution mass spectroscopies and elemental analyses.

Binding of α-Amino Acid Esters, *β*-Amino Ethers, and Amines by a Series of Zinc Bilindiones. UV−vis spectral changes of ZnBDs in CH_2Cl_2 and $CHCl_3$ at 288 K upon addition of α-amino acid esters, *β*-amino alcohol methyl ethers, and amines exhibited saturation behaviors, indicating that these amines were complexed with ZnBDs. As representative examples, UV−vis spectral changes of **2** in CH_2Cl_2 upon addition of L-Trp-OMe and of **4** in CH_2Cl_2 upon addition of L-Leu-OMe are shown in Figure 1. The binding constants were determined by least-squares analysis of the absorbance changes at 346 and 402 nm for **1**−**3** (1.25×10^{-5}−4.51×10^{-5} M) and at 702 and 770 nm for **4**−**8** (2.97×10^{-5}−4.50×10^{-5} M) as a function of guest concentrations 0−0.85 mM for **1**−**3** and 0−171 mM for **4**−**8** and are summarized in Table 1. The spectral changes showed isosbestic points (at 378, 458, and 678 nm for **1**, 370 and 446 nm for **2**, 322, 378, and 460 nm for **3**, and 320−322 and 796−816 nm for **4**−**8**) and fitting of the changes to the calculated curve based on 1:1 complexation was satisfactory.

(16) For preliminary account of this work, see: Mizutani, T.; Yagi, S.; Honmaru, A.; Ogoshi, H. *J. Am. Chem. Soc.* **1996**, *118*, 5318−5319.

(17) (a) Shrout, D. P.; Lightner, D. A. *Synthesis* **1990**, 1062. (b) Shrout, D. P.; Puzicha, G.; Lightner, D. A. *Synthesis* **1992**, 328.

(18) (a) Fuhrhop, J.-H.; Salek, A.; Subramanian, J.; Mengersen, C.; Besecke, S. *Liebigs Ann. Chem.* **1975**, 1131−1147. (b) Fuhrhop, J.-H.; Kruger, P.; Sheldrick, W. S. *Liebigs Ann. Chem.* **1977**, 339. The oxoniaporphyrin was then cleaved to yield a 19-methoxy-1-bilinone derivative: (c) Fuhrhop, J.-H.; Kruger, P. *Liebigs Ann. Chem.* **1977**, 360.

Scheme 2

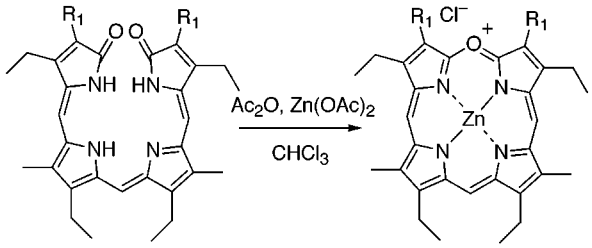

15a: $R_1 = CH_3$
15b: $R_1 = CH_2CH_2OAc$
15c: $R_1 = CH_2CH_2OH$
15d: $R_1 = CH_2CH_2CH_3$

16a: $R_1 = CH_3$
16b: $R_1 = CH_2CH_2OAc$
16c: $R_1 = CH_2CH_2CH_3$

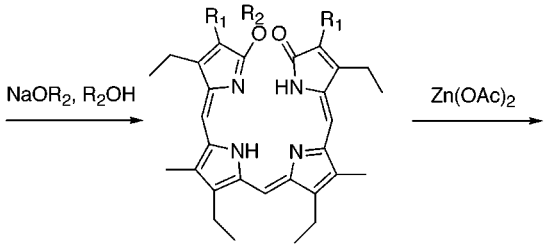

17a: $R_1 = CH_3$, $R_2 = CH_3$
17b: $R_1 = CH_2CH_2OAc$, $R_2 = CH_3$
17c: $R_1 = CH_2CH_2OH$, $R_2 = CH_3$
17e: $R_1 = CH_2CH_2CH_3$, $R_2 = CH_3$
17d: $R_1 = CH_3$, $R_2 = CH(CH_3)_2$

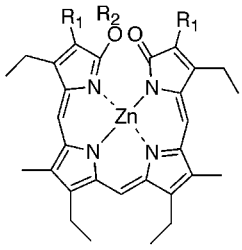

4: $R_1 = CH_3$, $R_2 = CH_3$
5: $R_1 = CH_2CH_2OH$, $R_2 = CH_3$
6: $R_1 = CH_2CH_2OAc$, $R_2 = CH_3$
7: $R_1 = CH_2CH_2CH_3$, $R_2 = CH_3$
8: $R_1 = CH_3$, $R_2 = CH(CH_3)_2$

For a comparative study, eight zinc bilindiones (**1**−**8**) were used as hosts. ZnBDs **1**−**3** have a lactim OH group, while **4**−**7** and **8** have a methyl group and an isopropyl group on the lactim oxygen, respectively. The substituents on the A- and D-rings are also varied: **1**, **4**, and **8** have 2,18-dimethyl, **2** and **5** have 2,18-bis(2-hydroxyethyl), and **3** and **6** have 2,18-bis(2-acetoxyethyl) groups. Guests used were methyl, dimethyl, benzyl, or naphthylmethyl esters of α-amino acids, several chiral amines **18**−**22**, and β-amino alcohol methyl ethers **23**−**24**.[19] The

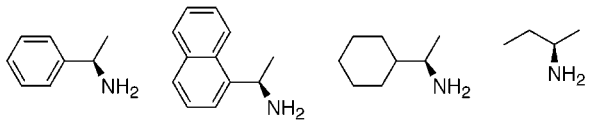

(*R*)-**18** (*R*)-**19** (*R*)-**20** (*R*)-**21**

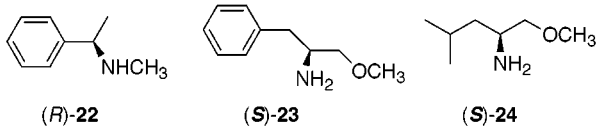

(*R*)-**22** (*S*)-**23** (*S*)-**24**

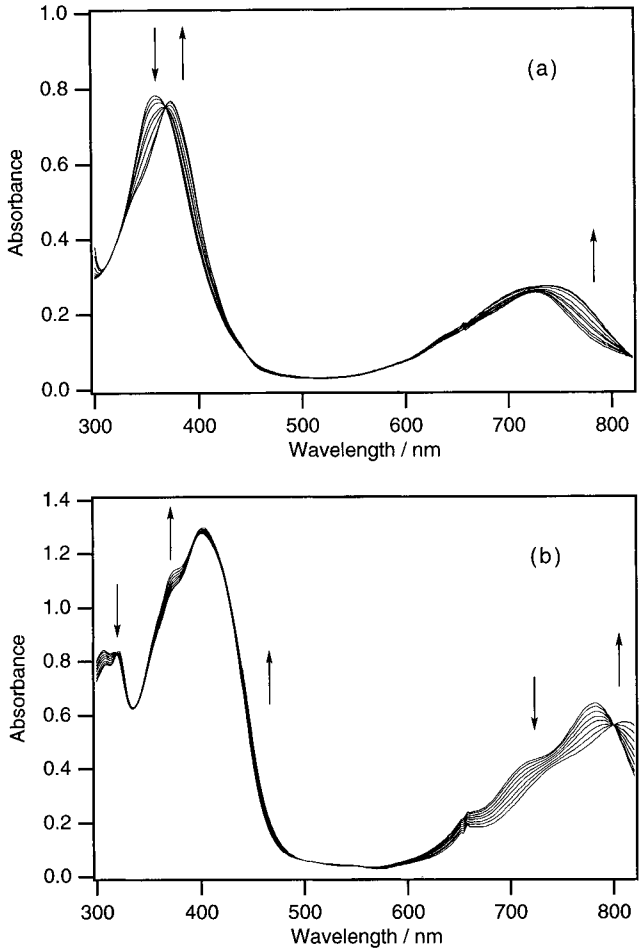

Figure 1. UV−vis spectral changes of (a) a solution of **2** (2.26×10^{-5} M) in CH_2Cl_2 upon addition of L-Trp-OMe (0, 3.12×10^{-6}, 6.22×10^{-6}, 1.38×10^{-5}, 1.83×10^{-5}, 2.99×10^{-5}, 5.95×10^{-5}, 1.18×10^{-4}, and 1.61×10^{-4} M) at 288 K and (b) a solution of **4** (3.79×10^{-5} M) in CH_2Cl_2 upon addition of L-Leu-OMe (0, 8.16×10^{-4}, 2.42×10^{-3}, 4.78×10^{-3}, 7.81×10^{-3}, 1.55×10^{-2}, 3.08×10^{-2}, and 8.20×10^{-2} M) at 288 K.

zinc bilindiones **1**−**3** were less stable than **4**−**8** in CH_2Cl_2 and $CHCl_3$ solutions: **1**−**3** with a 19-OH group were gradually demetalated in a few hours and the demetalation was suppressed by the addition of amino acid esters or amines. No demetalation was observed for 19O-alkylated ZnBDs **4**−**8** within a few days in the solution.

The binding constants for amines and amino acid esters showed a considerable diversity depending on the combinations of substituents at the 2,18-positions (R_1) and the 19O-position (R_2). The effects of the substituents can be summarized as follows. (1) The 2-hydroxyethyl groups at the 2,18-positions strongly enhanced the binding affinity of ZnBDs, and the binding constants of guests by **2** were increased by a factor of 10 as compared to the corresponding binding constants of **1**. (2) Protection of the hydroxy groups by acetyl groups reduced the binding constants to the magnitude comparable to those of parent

(19) Guests used and their abbreviations: glycine methyl ester (Gly-OMe), alanine methyl ester (Ala-OMe), valine methyl ester (Val-OMe), leucine methyl ester (Leu-OMe), leucine benzyl ester (Leu-OBz), leucine 1-naphthylmethyl ester (Leu-ONp), isoleucine methyl ester (Ile-OMe), methionine methyl ester (Met-OMe), aspartic acid dimethyl ester (Asp-$(OMe)_2$), glutamic acid dimethyl ester (Glu-$(OMe)_2$), phenylalanine methyl ester (Phe-OMe), tryptophan methyl ester (Trp-OMe), phenylglycine methyl ester (PhGly-OMe), and proline methyl ester (Pro-OMe).

Table 1. Binding Constants (K_{288}, M^{-1}) for a Series of Zinc Bilindione Derivatives (1−8) of Various Amino Acid Esters and Amines in CH_2Cl_2 at 288 K[a,b]

guest	**1**	**2**	**3**	**4**	**5**	**6**	**7**	**8**
L-Ala-OMe	3480	34400	4170	90	230	194	99	79
L-Val-OMe	3410	29700	3740	55	177	119	67	41
L-Leu-OMe	4780	45500	4750	106	271	210	111	98
L-Ile-OMe	4560	45500	3960	91	248	200	109	64
L-Met-OMe	1770	18600	1760	66	161	143	80	49
L-Asp-$(OMe)_2$	1640	16700	2850	53	145	128	70	44
L-Glu-$(OMe)_2$	890	11600	636	20	111	88	53	33
L-Phe-OMe	3690	29000	4490	96	231	108	117	72
L-Trp-OMe	7010[c]	89700[d]	13700	115	631	191	*g*	64
D-PhGly-OMe	1940	14300	4150	76	200	153	78	55
(*R*)-**18**	13700[e]	190000	13760	205	546	415	209	133
(*R*)-**19**	21600	368000	37700	296	882	631	324	171
(*R*)-**20**	277000	$>10^6$	331700	600	1980	1330	661	457
(*S*)-**21**	79700	*f*	*f*	454	*f*	*f*	*f*	*f*

[a] For abbreviations, see footnote 19. Standard deviations for the curve fitting were typically 2% and less than 5%, except for the **1**−**20**, **2**−**20**, **3**−**20**, **2**−**18**, and **2**−**19** complexes. [b] K_{288} (**2**−Gly-OMe) = 38 000 M^{-1}, K_{288} (**1**−Pro-OMe) = 26 400 M^{-1}, K_{288} (**1**−(*R*)-**22**) = 1970 M^{-1}, K_{288} (**1**−(*S*)-**23**) = 49 400 M^{-1}, K_{288} (**1**−(*S*)-**24**) = 130 000 M^{-1}, K_{288} (**4**−Pro-OMe) = 45 M^{-1}, K_{288} (**4**−(*R*)-**22**) = 4.4 M^{-1}, K_{288} (**4**−(*S*)-**23**) = 300 M^{-1}, K_{288} (**4**−(*S*)-**24**) = 370 M^{-1}. [c] K_{288} (**1**−D-Trp-OMe) = 6550 M^{-1}. [d] K_{288} (**2**−D-Trp-OMe) = 89 500 M^{-1}. [e] K_{288} (**1**−(*S*)-**18**) = 13 600 M^{-1}. [f] Not determined. [g] During titration, demetalation occurred.

1. (3) The 19O-methyl group also suppressed the binding, with the binding constants of **4** decreased by a factor of ca. 50 as compared to **1**. The binding affinity enhanced by the 2-hydroxyethyl groups was seen for all of the guests irrespective of the existence of a hydrogen-bonding site in the guest. One can explain the high binding affinity of **2** by assuming that the 2-hydroxyethyl group forms intramolecular hydrogen bonding to the lactam carbonyl, decreasing the electron density of zinc, and activating the zinc as a Lewis acid. The inhibitory effects of the 19O-alkyl group on the binding appear to originate from (1) increased electron density on zinc due to the electron-donating alkyl group and (2) loss of polar interactions, possibly hydrogen bonding, between the lactim OH group and the amino group of guest (vide infra, Figure 8).

The amines **18**−**21** were more tightly bound to **1**−**8** than the amino acid esters. The same trend was seen for the binding by zinc porphyrin derivatives.[20] This trend can be ascribed to the higher basicity of the amino group of amines than that of α-amino acid esters. Secondary amines such as **22** and Pro-OMe were bound weakly to **4**, while Pro-OMe was tightly bound to zinc porphyrin.[20] This weak affinity for secondary amines may reflect more crowded geometry around zinc in zinc bilindione compared to zinc porphyrin.

UV−vis titration experiments showed that addition of amino alcohols such as leucinol to **4** caused demetalation, and the binding affinity toward amino alcohols could not be determined. Instead, binding of amino alcohol methyl ethers was studied. Phenylalaninol methyl ether (**23**) and leucinol methyl ether (**24**) showed large binding constants comparable to those of amines.

Circular Dichroism Studies on Helical Chirality Induction. ZnBDs **1**−**8** exist as racemates in a solution and exhibit no Cotton effects. Addition of chiral α-amino acid methyl esters, *β*-amino ethers, and amines to solutions of **1**−**8** in CH_2Cl_2 or $CHCl_3$ induced Cotton effects in the zinc bilindione bands. The induced Cotton effects were characteristic of a helical structure of the chromophore.[11d,21] As a representative example, the CD spectra of a solution of **4** and Leu-OMe in CH_2Cl_2 at 288 and 223 K are shown in Figure 2. The positive Cotton effect at the higher energy band and the negative one at the lower energy band revealed that L-Leu-OMe induced *M*-helicity in the framework of **4**.[21] The values of differential dichroic absorption ($\Delta\epsilon_{288}$, $\Delta\epsilon_{223}$) of the higher energy band for ZnBD-amino acid ester (or amine) complexes in CH_2Cl_2 at 288 and 223 K are listed in Tables 2 and 3, respectively, where the observed differential dichroic absorption was corrected for the concentrations of the complexes. In all cases, Cotton effects with an opposite sign were observed at the lower energy band as typically shown in Figure 2.

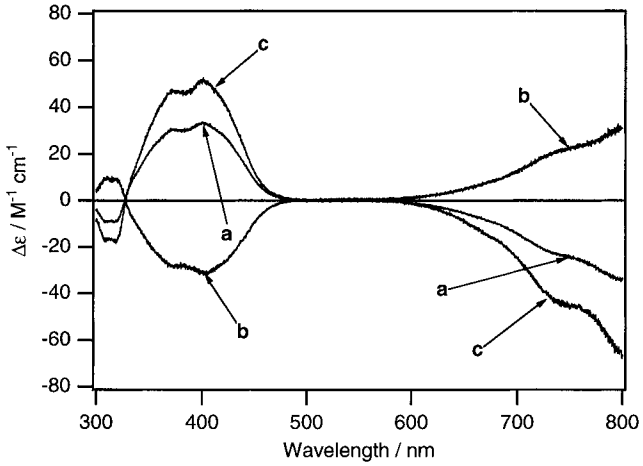

Figure 2. CD spectra of the **4**−Leu-OMe complex in CH_2Cl_2. (a) L-Leu-OMe at 288 K, (b) D-Leu-OMe at 288 K, and (c) L-Leu-OMe at 223 K. [**4**] = 3.79×10^{-5} M, [D/L-Leu-OMe] = 8.20×10^{-2} M at 288 K, 2.77×10^{-2} M at 223 K.

Typical titration curves of UV−vis and CD spectra for formation of the **2**−L-Phe-OMe complexes are shown in Figure 3. The induced Cotton effects developed concurrently as the UV−vis spectral changes, showing that the complexation with L-Phe-OMe directly induced the helical chirality in the zinc bilindione. The binding constants of ZnBD **2** determined by UV−vis (K_{vis}) and those

(20) Mizutani, T.; Ema, T.; Yoshida, T.; Kuroda, Y.; Ogoshi, H. *Inorg. Chem.* **1993**, *32*, 2072.

(21) (a) Bulke, M. J.; Pratt, D. C.; Moscowitz, A. *Biochemistry* **1972**, *11*, 1, 4025−4031. (b) Blauer, G.; Wagniere, G. *J. Am. Chem. Soc.* **1975**, *97*, 1949−1954. (c) Wagniere, G.; Blauer, G. *J. Am. Chem. Soc.* **1976**, *98*, 7806−7810. (d) Scheer, H.; Formanek, H.; Schneider, S. *Photochem. Photobiol.* **1982**, *36*, 259−272.

Table 2. Differential Dichroic Absorption ($\Delta\epsilon_{288}$/M^{-1} cm^{-1}) in the Higher Energy Band of Complexes between 1−8 and Various Chiral Amino Acid Esters and Amines in CH_2Cl_2 at 288 K[a]

guest	**1**	**2**	**3**	**4**	**5**	**6**	**7**	**8**
L-Ala-OMe	<1.5	<1	1.7	32.2	22.8	29.4	35.0	29.1
L-Val-OMe	19.8	15.4	18.4	32.5	18.3	26.2	28.1	28.6
L-Leu-OMe	16.0	13.2	14.4	37.3	31.3	36.3	39.0	36.9
L-Ile-OMe	22.9	21.4	18.9	46.8	33.4	40.0	45.3	45.5
L-Met-OMe	13.0	12.2	12.2	31.4	25.7	32.1	35.1	30.7
L-Asp-$(OMe)_2$	2.3	5.0	3.7	46.1	32.6	42.2	49.1	42.4
L-Glu-$(OMe)_2$	3.3	2.9	−3.1	30.2	18.3	25.5	29.7	23.7
L-Phe-OMe	18.3	21.8	21.2	36.7	30.3	37.1	37.8	33.8
L-Trp-OMe	14.9[b]	14.6[c]	16.3	46.6	16.8	26.2	*e*	40.4
D-PhGly-OMe	−19.0	−20.2	−17.2	−38.8	−28.7	−33.2	−38.7	−35.3
(*R*)-**18**	13.4[d]	14.4	12.1	0	<2.7	−2.7	−3.9	0
(*R*)-**19**	16.3	16.1	12.8	28.3	24.1	25.3	24.5	34.9
(*R*)-**20**	6.2	16.1	5.0	7.9	3.3	4.1	5.4	8.1
(*S*)-**21**	0	*f*	*f*	6.1	*f*	*f*	*f*	*f*

[a] $\Delta\epsilon_{288}$ (**1**−L-Pro-OMe) = −6.1, $\Delta\epsilon_{288}$ (**1**−(*R*)-**22**) = 3.8, $\Delta\epsilon_{288}$ (**1**−(*S*)-**23**) = 4.8, $\Delta\epsilon_{288}$ (**1**−(*S*)-**24**) = −4.5, $\Delta\epsilon_{288}$ (**4**−L-Pro-OMe) = −6.5, $\Delta\epsilon_{288}$ (**4**−(*R*)-**22**) = −6.1, $\Delta\epsilon_{288}$ (**4**−(*S*)-**23**) = 9.0, $\Delta\epsilon_{288}$ (**4**−(*S*)-**24**) = −3.9. [b] $\Delta\epsilon$ (**1**−D-Trp-OMe) = −14.5. [c] $\Delta\epsilon$ (**2**−D-Trp-OMe) = −15.2. [d] $\Delta\epsilon$ (**1**−(*S*)-**18**) = −13.8. [e] Not determined because the stoichiometry of the complex other than 1:1 also contribute to the ICD. [f] Not determined.

Table 3. The Differential Dichroic Absorption ($\Delta\epsilon$/M^{-1} cm^{-1}),[a] the Binding Constants for Each Diastereomer (K_{223}, K_{223}'/M^{-1}),[b] and Diastereomeric Excess (de) for the Complexes between Hosts 4 and 8 and Various Chiral Amino Acid Esters and Amines in Dichloromethane at 223 K

host	guest	$\Delta\epsilon_{223}$	K_{223}	$K_{223'}$	de (%)[c]
4	L-Ala-OMe	52.9	5050	2790	42
4	L-Val-OMe	47.3	2450	1060	42
4	L-Leu-OMe	51.4	4750	1980	37
4	L-Leu-OBz	*d*	6720	2960	41
4	L-Leu-ONp[b]	*d*	4960	2310	41
4	L-Ile-OMe	60.9	5170	1780	46
4	L-Trp-OMe	87.7	*e*	*e*	73
4	L-Phe-OMe	60.9	6350	2150	57
4	L-Asp-$(OMe)_2$	83.8	9260	2150	70
4	L-Glu-$(OMe)_2$	60.5	4010	1290	51
4	D-PhGly-OMe	−60.7	2590	980	42
4	(*S*)-**23**	15.3	52400	45100	13
4	(*S*)-**24**	−14.7	41500	42300	9
4	(*R*)-**18**	−12.5	7750	6480	14
4	(*R*)-**19**	37.7	11900	6680	30
4	(*R*)-**20**	5.1	32700	29700	6
8	L-Leu-OMe	47.8	4150	1980	36
8	L-Trp-OMe	78.1	*e*	*e*	70
8	L-Phe-OMe	55.8	4120	1470	46
8	(*R*)-**18**	−14.3	7490	6420	10
8	(*R*)-**19**	42.6	13200	7410	31
8	(*R*)-**20**	3.8	23300	20700	2

[a] The values of $\Delta\epsilon$ at 399−405 nm for **4** and 398−408 nm for **8** are reported. [**4** or **8**] = 3.2 × 10^{-5}−4.5 × 10^{-5} M, [guest] = 23−33 mM. [b] Binding constants K' and K'' are defined in Scheme 3. The binding constants were determined by the ^{1}H NMR titration at 223 K. [c] Determined by the ^{1}H NMR signal integration in CD_2Cl_2 at 223 K. [**4** or **8**] = 2.2 mM, [guest] = 14−62 mM. Under these conditions more than 98% of **4** was complexed with the guest. [d] Not determined. [e] Not determined owing to the anomalous dependence of chemical shift displacements on Trp-OMe concentrations.

determined by CD spectroscopy (K_{CD}) in CH_2Cl_2 at 288 K were the following: L-Val-OMe, K_{vis} = 29 700 ± 1200, K_{CD} = 28 700 ± 2900 M^{-1}; L-Phe-OMe, K_{vis} = 29 000 ± 1100, K_{CD} = 36 600 ± 6300 M^{-1}; L-Trp-OMe, K_{vis} = 89 700 ± 5100, K_{CD} = 68 300 ± 3900 M^{-1}. Considering relatively large standard deviations for K_{CD}, the agreement between K_{vis} and K_{CD} was satisfactory.

As described later in this paper, the values of $\Delta\epsilon$ directly reflected the enantiomeric excess of ZnBDs complexed with guest. Comparison of $\Delta\epsilon$ values in Table 2 indicates that helical chirality induction behaviors were similar among **1**−**3** and among **4**−**8**. Helical chirality was induced in **4** efficiently by aromatic amino acid esters, Asp-$(OMe)_2$, and Ile-OMe. The large value of $\Delta\epsilon$ for Asp-$(OMe)_2$ was unexpected: **4** can distinguish two similar groups attached to the chiral carbon, COOMe and CH_2COOMe.

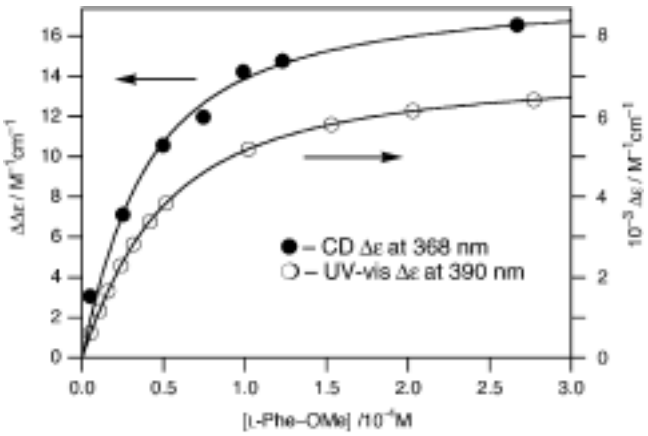

Figure 3. UV−vis titration and CD titration curves. To a solution of **2** in CH_2Cl_2 was added L-Phe-OMe at 288 K. Peaks at 390 nm in the UV−vis spectra and at 368 nm in the CD spectra were monitored as a function of [L-Phe-OMe]. [**2**] = 2.49 × 10^{-5} M for UV−vis and 1.98 × 10^{-5} M for CD.

Table 2 shows that there are interesting differences in helical chirality induction between **1** and **4**. Ala-OMe induced almost no Cotton effects in **1**, while it induced distinct Cotton effects in **4** as efficiently as Val-OMe and Leu-OMe. Asp-$(OMe)_2$ and Glu-$(OMe)_2$ induced strong Cotton effects in **4**, while they induced small Cotton effects in **1**. Thus, the 19O-alkyl groups affected not only the overall binding affinity but also the interactions inducing helical chirality. An important structural difference between **1** and **4** is that the polarity of the D ring is reversed: the terminal D ring of **1** has a positively charged hydrogen, while that of **4** a negatively charged oxygen. For efficient helical chirality induction in **4**, a repulsive interaction between the negatively charged terminal D or A ring of ZnBDs and the COOR group of the guest appears to be important.

NMR Studies of the Complexation and Chiral Induction. The ^{1}H NMR signals of **4** were assigned by NOESY experiments. The cross-peaks were observed between the protons as shown in Figure 4, which

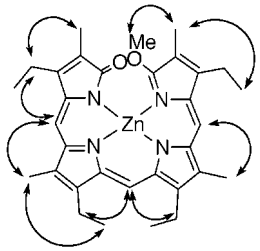

Figure 4. NOESY correlations in the ^{1}H NMR of **4** in CD_2Cl_2 at 298 K.

Scheme 3

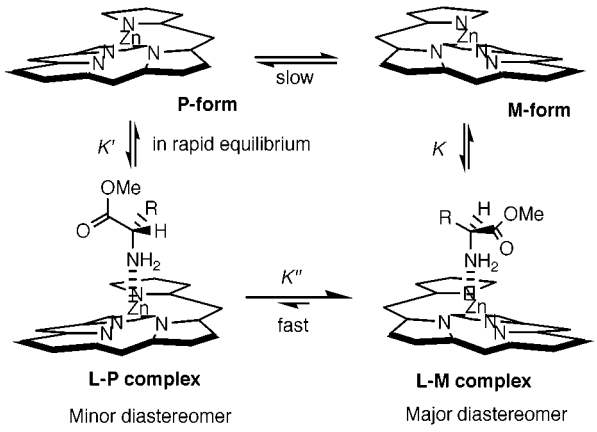

established that **4** assumed a helical conformation along with complete assignments of these signals.[22]

Addition of **4** to a solution of **19** in dry $CDCl_3$ at 296 K caused the complexation-induced shift (CIS) of the NH_2 protons of **19** from 1.50 to 3.00 ppm with some signal broadening, where 46% of **4** was complexed with **19**. This result clearly indicates that the amino group of **19** was coordinated to the zinc of **4**.

The equilibria shown in Scheme 3 should be considered to explain ^{1}H NMR spectral behaviors of a solution of **4**−guest complexes. Only averaged signals between complexed **4** and free **4** were observed in the temperature range of 223−288 K, indicating that complex formation and dissociation were fast on the NMR time scale over this temperature range. Thus, at room temperature, only one set of signals appeared. When the solution was cooled, however, these signals decoalesced into two sets of signals and two sets of well-resolved signals appeared at 223 K, showing that the helix inversion between guest−*P*-**4** and guest−*M*-**4** became slow on the NMR time scale at low temperatures. Addition of excess guest caused the coalescence of the signals, indicating that the helix inversion was catalyzed by guest. The details of kinetic aspects will be reported elsewhere.

Because two diastereomers gave resolved signals at low temperature, ^{1}H NMR at 223 K afforded valuable information on diastereomeric excess of the complexes. Typical ^{1}H NMR spectra of solutions of **4** and L-Leu-OMe in CD_2Cl_2 at 223 K are shown in Figure 5. Upon addition of a small amount of L-Leu-OMe, the 5-H, 10-H, 15-H and MeO signals of **4** split into two with almost the same intensity. When more L-Leu-OMe was added, these signals were shifted and one set of the signals became dominant, which was in this case assigned to the L-Leu-

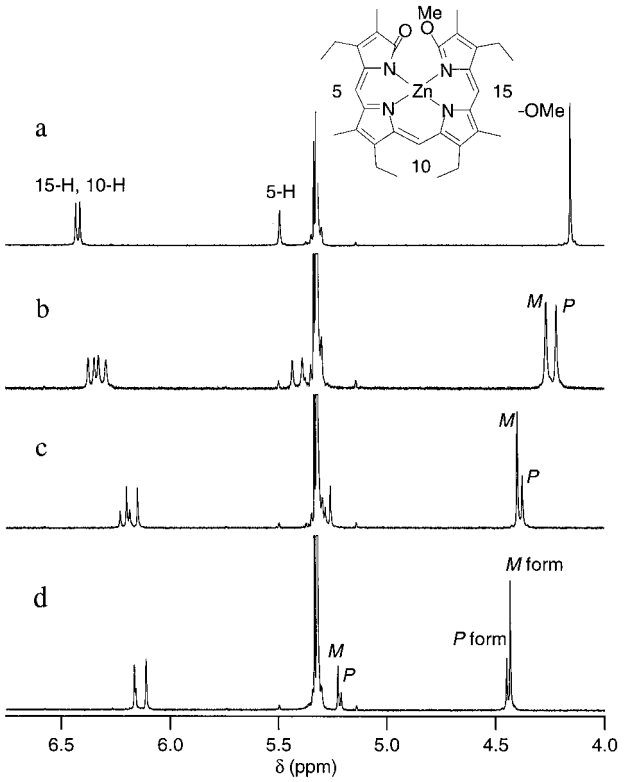

Figure 5. 500 MHz ^{1}H NMR spectra of solutions of 2.46×10^{-3} M of host **4** in the presence of varying concentrations of L-Leu-OMe in CD_2Cl_2 at 223 K. The concentrations of Leu-OMe were (a) 0, (b) 9.03×10^{-4}, (c) 3.56×10^{-3}, and (d) 2.51×10^{-2} M.

OMe−*M*-**4** complex on the basis of the sign of Cotton effects of the complex. From the integration of each of the 19-MeO signals in the ^{1}H NMR spectra taken at 223 K, the diastereomeric excesses (de) were determined for the **4**−chiral guest complexes. Similarly, on the basis of the integration of 10-H and 15-H signals, the de was determined for **8**−chiral guest complexes. The values of de are listed in Table 3.

The binding constants of chiral guest to *M*-**4** and *P*-**4** (K_{223}, K'_{223}) were determined by the ^{1}H NMR titration experiments at 223 K, where the complexation-induced shifts of each of the 19-methoxy signals were monitored as a function of guest concentrations (Table 3). For **8**, the complexation-induced shifts of 10-H and 15-H were monitored. By using the binding constants, diastereomeric excesses were calculated according to the equation, $de = (K_{223} - K'_{223})/(K_{223} + K'_{223}) \times 100$ (%), which were mostly in good agreement with those determined by the integration of the 19-MeO signal.[23]

In Figure 6 are plotted the values of $\Delta\epsilon_{223}$ at 400 nm for the **4**−guest complexes determined by CD spectroscopy against the diastereomeric excesses determined by ^{1}H NMR signal integration at 223 K. A good linear correlation indicates that the induced Cotton effects originated from the distribution over the two enantiomeric helical conformations and any direct electromagnetic coupling between the guest chromophore and the bilindione chromophore makes a negligibly small contribution to the induced CD. Thus, the magnitude of Cotton

(22) Sturrock, E. D.; Bull, J. R.; Kirsch, R. E.; Pandey, R. K.; Senge, M. O.; Smith, K. M. *J. Chem. Soc., Chem. Commun.* **1993**, 872−874.

(23) Diastereomer excess determined by signal integration and that by the binding constants agreed within 15% except for the **4**−Ala-OMe, **4**−**18**, **4**−**20**, **8**−**18**, and **8**−**20** complexes.

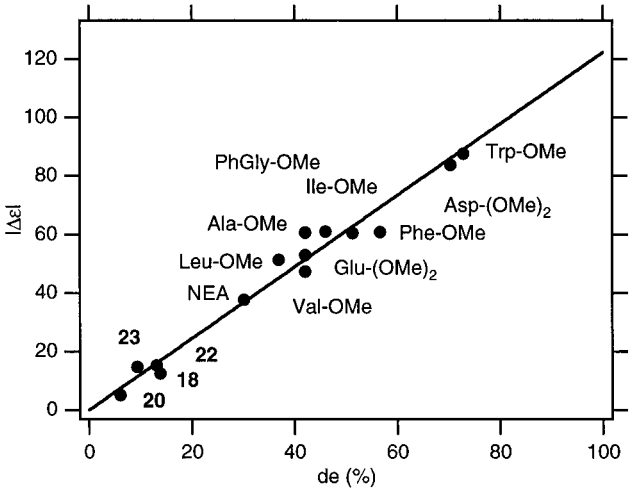

Figure 6. Plot of $|\Delta\epsilon|$ at the higher energy band maxima in the CD spectra against diastereomeric excesses (de) determined by NMR peak integration. Both the CD and the NMR spectra were recorded at 223 K in CH_2Cl_2 and CD_2Cl_2, respectively. [**4**] = 3.5×10^{-5}−4.2×10^{-5} M, [guest] = 0.025−0.049 M for the CD studies. For NMR conditions, see footnote c to Table 3.

effects is a good measure of diastereomeric excesses and the efficiency of helical chirality induction. A similar plot for the **8**−guest complexes also gave a good linear correlation with almost the identical slope.[24] Therefore, **4** and **8** showed quite similar behavior both in the helical chirality induction and induced CD.

Complexation-induced shifts of **4** upon addition of various guests are summarized in Figure 7. The upfield shifts of the 10-H proton of the major diastereomer induced by Phe-OMe and Trp-OMe revealed that the aromatic moiety of the guest was stacked with the B or C ring in the major diastereomer. Perturbation in the 5-H proton by the aromatic guests was small. The resonances of the indole 2-H and N−H of Trp-OMe were also shifted upfield upon complexation (vide infra), consistent with the stacking of the indole ring on bilindione. When complexed with **19**, the resonance of 5-H of **4** in the major diastereomer was shifted upfield, while that of 15-H of the minor one shifted upfield, indicating that the naphthyl group took different positions in the two diastereomers. In the ^{1}H NMR spectra of the **4**−Leu-ONp complex and the **4**−Leu-OBz complex, there was no particular difference in the pattern of the complexation-induced shifts of 5-, 10-, and 15-H and 19-OMe protons when compared to that of the **4**−Leu-OMe complex. These results for Leu-OR (R = Me, benzyl, and 1-naphthylmethyl) strongly suggest that the COOR group is not in van der Waals contact with the bilindione framework and is away from it.

Comparison of the ^{1}H NMR spectra of **4**−guest complexes ([**4**] = [guest] = 22 mM) in CD_2Cl_2 at 223 K with those of free guest indicated that the H-2 proton of indole of Trp-OMe and the ortho protons of phenyl of Phe-OMe were shifted upfield by 0.61 and 0.5 ppm, respectively. For Leu-OMe, no characteristic shift was observed. These chemical shift displacements suggest that the aromatic rings in the side chain of Trp-OMe and Phe-OMe are stacked with the bilindione.

(24) The slope of the plot for **4** was 121.8 and that for **8** was 118.5.

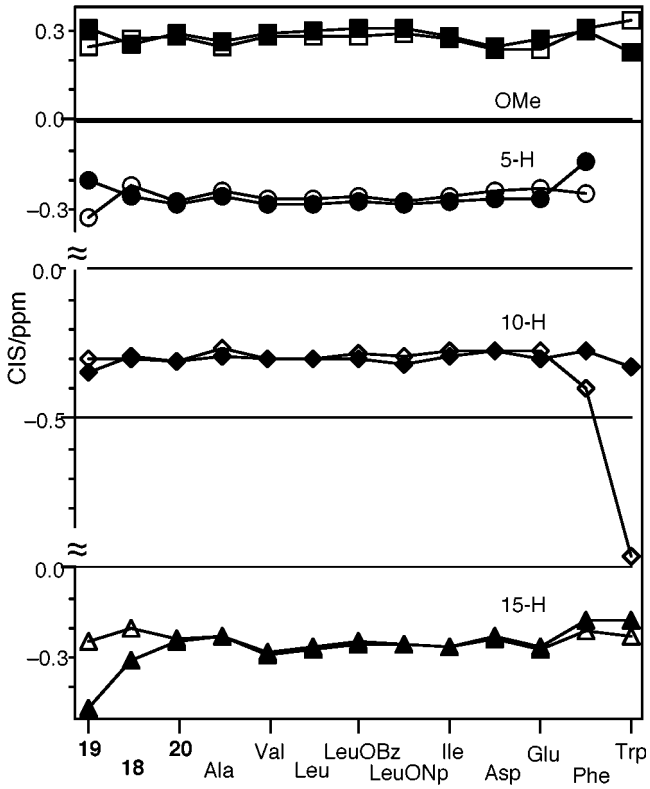

Figure 7. Complexation-induced shifts of 5-H, 10-H, 15-H, and MeO signals of **4** in the ^{1}H NMR spectra in CD_2Cl_2 at 223 K upon addition of various guests, (*R*)-**18**−**20**, L-Ala-OMe, L-Val-OMe, L-Leu-OMe, L-Leu-OBz, L-Leu-ONp, L-Ile-OMe, L-Asp-$(OMe)_2$, L-Glu-$(OMe)_2$, L-Phe-OMe, and L-Trp-OMe. Open squares, circles, and triangles represent the major *M*-isomer, while filled squares, circles, and triangles the minor *P*-isomer.

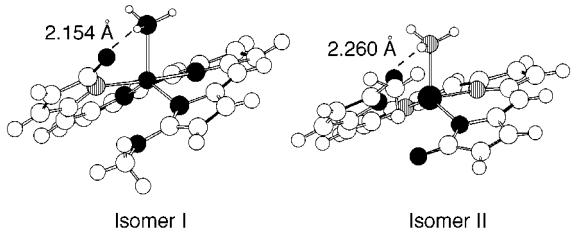

Figure 8. Two isomers of the [1,19-bilindionato]zinc−NH_3 complex optimized by ab initio MO calculations at the HF/6-311G level.

As shown in Figure 8, there are two possible isomers of ZnBD−NH_2R complexes, one with the NH_2 group coordinated from the A ring side (isomer I), the other from the D ring side (isomer II). A similar behavior between **4** and **8** in the binding affinity and helical chirality induction (Tables 1−3) implies that isomer I is favorable. The ab initio calculations of the [19-methoxy-(21*H*,24*H*)-1-bilinonato(2−)-N^{21},N^{22},N^{23},N^{24}]zinc(II)−NH_3 complex were performed at the 3-21G, 6-311G, and B3LYP levels. On the basis of the 3-21G-optimized geometry, isomer I was more stable than isomer II by 1.8 kcal/mol. Similar results were obtained by using a larger basis set: on the basis of the 6-311G-optimized geometry, isomer I was more stable than isomer II by 1.2 kcal/mol (6-311G) or by 1.9 kcal/mol (B3LYP). In Figure 8, the 6-311G-optimized structures are shown. The (N−)H to O distances were 2.154 Å (isomer I) and 2.260 Å (isomer II), and the N−H−O bond angles were

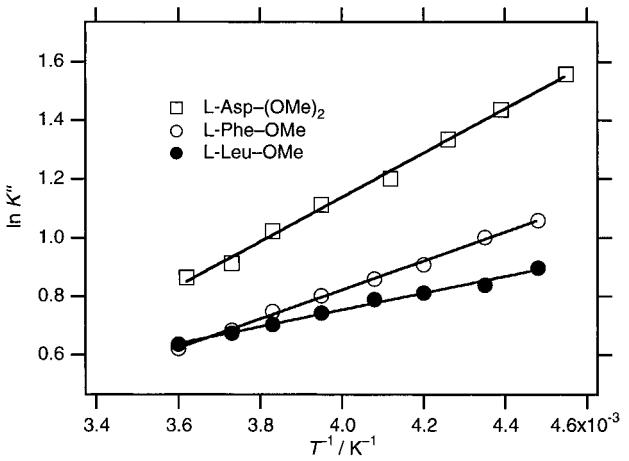

Figure 9. Plot of ln K'' against T^{-1} for the **4**−L-Asp-$(OMe)_2$ complex, the **4**−L-Phe-OMe complex, and the **4**−L-Leu-OMe complex. K'' is the equilibrium constant between the two diastereomers, the L-guest−*M*-**4** and L-guest−*P*-**4** complexes (Scheme 3).

144.5° (isomer I) and 142.9° (isomer II), showing strong hydrogen-bonding between the NH_3 ligand and the bilindione oxygen. We suggest that isomer I is favorable because a C═O group is a better hydrogen bond acceptor than a MeO group.

The ^{1}H NMR spectral features of the complexes between **1**−**3** and chiral guests differed from those between **4**−**8** and chiral guests in two respects. (1) Complex formation and complex dissociation were slow on the NMR time scale even at 288 K, and thus the signals from the free host and the complexed host appeared separately. (2) Tautomeric isomerization of the lactim OH proton also affected the dynamics of the ^{1}H NMR spectra, complicating analysis of the diastereomer distribution based on the variable-temperature NMR. Therefore, the diastereomeric excess of the complexes between **1**−**3** and chiral guest could not be determined by ^{1}H NMR studies.

Temperature Dependence of the Binding and Chiral Induction. The binding constants of amino acid esters and amines by ZnBDs **4** and **8** in CH_2Cl_2 at 223 K were larger than those at 288 K by a factor of 25−56. Therefore, the binding was enthalpically driven, and the estimated values of $\Delta H°$ were −6.3 to −7.9 kcal/mol. This is close to the value of $\Delta H°$ for complex formation between Leu-OMe and [2,3,7,8,12,13,17,18-octaethyl-5,10-bis(1-naphthyl)porphyrinato]zinc(II) in $CHCl_3$, which was reported to be −8.3 kcal/mol.[25]

The $\Delta\epsilon$ values of the **4**-guest complexes at 223 K were larger in magnitude than those at 288 K except for **20**, indicating that the helical chirality induction was also enthalpically driven. In Figure 9 is shown the plot of ln K'' against T^{-1} for the complexes between **4** and L-Asp-$(OMe)_2$, L-Phe-OMe, and L-Leu-OMe, where K'' represents the equilibrium constant between the two diastereomers (see Scheme 3). The values of K'' were obtained from the $\Delta\epsilon$ values at each temperature, taking advantage of the linear relationship between $\Delta\epsilon_{223}$ and diastereomeric excesses shown in Figure 6 and assuming the same relationship is valid at higher temperatures. From this plot, the enthalpy changes and entropy changes on going from L-guest−*P*-**4** to L-guest−*M*-**4** were obtained. For Asp-$(OMe)_2$, $\Delta H° = -1.50 \pm 0.04$ kcal/mol, $\Delta S° = -3.74 \pm 0.16$ cal/mol/K, for Phe-OMe, $\Delta H° = -0.98 \pm 0.02$ kcal/mol, $\Delta S° = -2.30 \pm 0.07$ cal/mol/K, and for Leu-OMe, $\Delta H° = -0.57 \pm 0.02$ kcal/mol, $\Delta S° = -0.78 \pm 0.09$ cal/mol/K. Thus, the negative sign of $\Delta H°$ indicated that the helical chirality induction was enthalpically driven and the enthalpic contribution was largest for the **4**−Asp-$(OMe)_2$ complex. As the origin of these negative enthalpy changes, attractive forces between the aromatic group in the side chain of guests and the bilindione B and C rings are expected to contribute helical chirality induction, when one considers the complexation-induced upfield shift of the 10-H proton of the **4**−Trp-OMe complex and the **4**−Phe-OMe complex of the major diastereomers in the ^{1}H NMR spectra. For Asp-$(OMe)_2$, dipole−dipole interaction between the ester group in the side chain and the bilindione framework could play a major role. In the case of Leu-OMe, an entropic contribution to helical chirality induction was larger than the others. Chiral induction in Ile-OMe showed a similar temperature dependence. It showed large $\Delta\epsilon$ at 288 K (46.8 $cm^{-1}M^{-1}$), while $\Delta\epsilon$ at 223 K was moderate (60.9 $cm^{-1}M^{-1}$). Therefore, for aliphatic amino acid esters, entropic forces contributed to helical chirality induction, resulting in comparatively higher helical chirality induction at higher temperature compared to aromatic amino acid esters.

Mechanism of Helical Chirality Induction. As discussed above, an aromatic group in *the side chain* of amino acid esters caused an upfield shift of 10-H of **4**, while an aromatic group (Ar) in *the ester group* ($COOCH_2$-Ar) scarcely influenced the CIS patterns (Figure 7), suggesting that the side chain is above the B and C rings and the ester group is away from the bilindione framework.

In Figure 10 is shown one of the possible structures of L-Ala-OMe−*M*-[19-methoxy-(21*H*,24*H*)-1-bilinonato(2-)-N^{21},N^{22},N^{23},N^{24}]zinc(II) complex optimized by semiempirical molecular orbital calculations at the PM3 level. The zinc complex of 19-methoxybilinone was used here as a model compound of **4**. This structure was obtained as the most stable one when 36 conformations were calculated at the PM3 level in which the amino group is coordinated to zinc and the substituents on the chiral carbon of L-Ala-OMe were rotated along the N−C_α bond by 10°, and other coordinates were optimized. The side chain group of amino acid ester (the methyl group in the case of Ala-OMe) is on the C ring, α-H on the B ring, the COOMe group nearly perpendicular to the bilindione framework, and the NH_2 group of Ala-OMe hydrogen bonded to the lactam carbonyl oxygen. This binding mode is consistent with the following features of chiral induction.

(1) α-Amino acid esters induced helical chirality more effectively than amines and amino alcohol methyl ethers, indicating that the COOR group of α-amino acid esters plays a crucial role in the helical chirality induction. The helical sense induced by amino acid esters was consistent, that is, all L-amino acid esters induced *M*-helicity except for the **1**−L-Pro-OMe complex, the **4**−L-Pro-OMe complex, and the **3**−L-Glu-$(OMe)_2$ complex at 288 K. On the other hand, the helical sense induced by amines and amino ethers was not consistent. For instance, (*R*)-**19** induced *M*-helicity, (*R*)-**18** induced almost no helical chirality, and (*R*)-**22** induced *P*-helicity in **4** at 288 K (Table 2). Therefore, the point chirality of the α-carbon of amino

(25) Mizutani, T.; Murakami, T.; Kurahashi, T.; Ogoshi, H. *J. Org. Chem.* **1996**, *61*, 539.

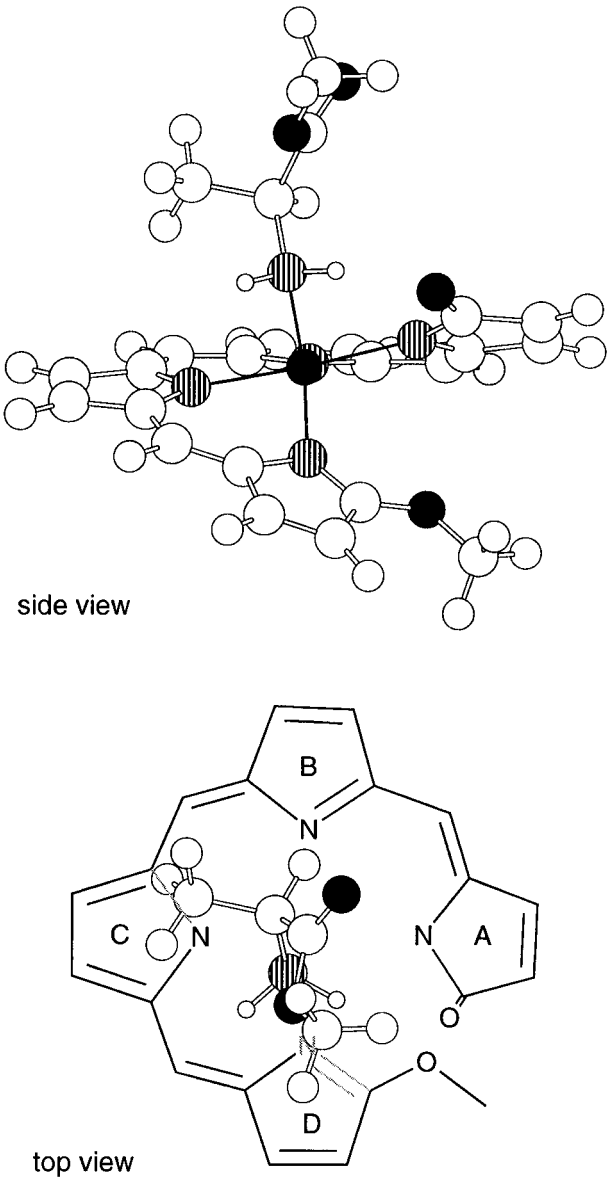

Figure 10. A possible structure for the *M*-[19-methoxy-(21*H*,24*H*)-1-bilinonato(2-)-*N*,^{21}N,^{22}N,$^{23}N^{24}$]zinc(II) complex−L-Ala-OMe complex, consistent with the ^{1}H NMR studies and helical chirality induction patterns. The geometry was optimized at the PM3 level.

acid esters directly determined the helical sense, while that is not the case for amines and amino ethers.[26]

(2) An aromatic group and a carbomethoxy group in the side chain of the guest made a significant contribution to the chiral induction, as seen in higher diastereomeric excesses for the complexes between **4** and Trp-OMe, Phe-OMe, Asp-$(OMe)_2$, and **19**.

(3) The binding constants of Leu-ONp and Leu-OBz by **4** at 223 K were similar to those of Leu-OMe. Diastereomeric excesses at 223 K were 41% for both of the aromatic esters, being similar to that of the methyl ester (37%). Compared with the high de of Trp-OMe and Phe-OMe, one can see that the aromatic group in *the side chain* helps induce helical chirality, while the aromatic group in *the ester group* had only minor effects on binding and chiral induction.

(26) Unusual behavior in helicity induction by Pro-OMe is readily understood if the coordination geometry around zinc should be much different for the secondary amine.

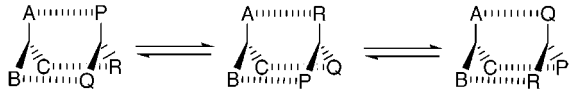

Figure 11. A simple model for interactions between two chiral molecules and three possible interaction modes.

Table 4. Interaction Energies between Recognition Groups of Two Chiral Molecules

	A (COOR)	B (side chain group)	C (α-H)
P (remote site)	a_{11}	a_{12}	a_{13}
Q (C ring)	a_{21}	a_{22}	a_{23}
R (B ring)	a_{31}	a_{32}	a_{33}

(4) Different patterns of helical chirality induction between **1** and **4** (Table 2) indicate that the polarity of the terminal rings of the bilindiones, possibly a repulsive force between the lactam ring of ZnBD and the ester group of guest, is one of the important factors for the chiral induction.

A Simple Model for Chirality−Chirality Interaction. If a variety of chirality can be quantitatively expressed in terms of a single measure, it would be useful for understanding chiral recognition.[27] One simple model is to consider a chiral molecule consisting of three elementary interacting groups, A, B, and C. Another chiral molecule has P, Q, and R. There are three possible binding modes between the two chiral molecules as shown in Figure 11. If the interaction energies for each pair of elementary parts are defined as in Table 4, then total energy E can be given by eqs 1−3

$$E = (e_1 \exp(-e_1/kT) + e_2 \exp(-e_2/kT) + e_3 \exp(-e_3/kT))/Z \quad (1)$$

$$Z = \exp(-e_1/kT) + \exp(-e_2/kT) + \exp(-e_3/kT) \quad (2)$$

$$e_1 = a_{11} + a_{22} + a_{33},\ e_2 = a_{12} + a_{23} + a_{31},\ e_3 = a_{31} + a_{21} + a_{32} \quad (3)$$

where e_1 is the energy for conformer 1, e_2 for conformer 2, e_3 for conformer 3, k Boltzman's constant, and T the absolute temperature. We simplify the model further by assuming that the conformation involving A−P pairing is much more stable than the others, then eq 1 can be reduced to eq 4.

$$E = e_1 \quad (4)$$

Similarly the energy E' for the complex between molecule ABC and enantiomeric molecule PQR, i.e., the corresponding diastereomer, is

$$E' = e_1' = a_{11} + a_{32} + a_{23} \quad (5)$$

The difference in energy between the diastereomers is

$$\Delta E = e_1 - e_1' = a_{22} + a_{33} - a_{23} - a_{32} \quad (6)$$

Therefore, the primary interaction energy term, a_{11}, is canceled and the energy difference between the diastereomers (ΔE) is determined by the difference in the second and the third interaction pairs.

We apply the above model to the bilindione chiral induction in a slightly modified way. We assume that the COOR group, the side chain group, and α-H consti-

(27) (a) Gilat, G. *J. Phys. A: Math. Gen.* **1989**, *22*, L545−L550. (b) Alvira, E. *Amino Acids (Vienna)* **1992**, *2*, 97−102. (c) Caravella, J. A.; Richards, W. G. *Eur. J. Med. Chem.* **1995**, *30*, 727−728.

tute three elementary groups of guest (A, B, and C). For ZnBD, based on the structure shown in Figure 10, we assume that P, Q, and R are a remote site from the bilindione framework, the B ring, and the C ring, respectively. Comparison of the helical chirality induction for a series of guest molecules indicated that the COOR group plays an important role. We thus regard the COOR group as group A. Then on the basis of the foregoing argument, group A preferentially occupies the remote site of **4**, namely site P. In the L-amino acid ester−*M*-**4** combination, the side chain group interacts with the C ring, and α-H with the B ring, while vice versa in the L-amino acid ester−*P*-**4** combination. ΔE can then be given by the difference between B−Q/C−R pairing energy and B−R/C−Q pairing energy. According to this model, the helical chirality induction originates from an unfavorable interaction between the side chain group of amino acid ester and the B ring in the "wrong" diastereomer complex and a favorable interaction between the side chain group and the C ring in the "correct" complex.

Conclusions. Point chirality of amino acid esters induced helical chirality in zinc bilindiones. Coordination of the NH_2 group of guest to Zn forced the substituents on the chiral carbon of amino acid esters to contact the helical surface of zinc bilindione. Comparative studies of the helical chirality induction in 19O-alkyl zinc bilindione **4** showed that the contribution of the substituents around point chirality to chiral induction decreased in the order COOR > side chain > α-H. By assigning the preferable sites for these substituents on zinc bilindione, we presented a model for point chirality−helical chirality intercoversion. Electrostatic repulsion between the COOR group and the bilindione lactam rings, i.e., complementarity of polarity, and an attractive stacking interaction between the aromatic group or the carbomethoxy group in the side chain of guest and the bilindione pyrrole rings were key forces for efficient chiral induction.

Experimental Section

General. ^{1}H NMR spectra (500 and 270 MHz) were recorded in $CDCl_3$, DMSO-d_6 and CD_2Cl_2, using TMS (0 ppm), DMSO (2.50 ppm), and $CHDCl_2$ (5.32 ppm) as internal standards, respectively. The NOESY spectrum was obtained for **4** at a concentration of 10 mM at 25 °C, where a pulse delay of 2.2 s and mixing time of 500 ms were employed. UV−vis absorption and circular dichroism spectra were recorded on the spectrometer equipped with a thermostated cell compartment. A cryostat (Oxford, DN1704) was used for CD spectral measurements at low temperatures. For the preparation of sample solutions for variable-temperature spectroscopic measurements, dichloromethane solutions of zinc bilindiones and/or guests were prepared in a volumetric flask at 15 °C, and the concentrations at low temperatures were calculated on the basis of the thermal expansion coefficient of dichloromethane (0.001 391 K^{-1}).[28] FAB mass spectra were obtained using 3-nitrobenzyl alcohol as a matrix. The optical rotation of 1-naphthylmethyl L-leucinate was recorded using a polarimeter with a sodium lamp (D-line, 589 nm) as a light source. Grid conformational search was performed using Sybyl 6.1, Tripos Inc. The ab initio MO calculations were performed by using the Gaussian 94 program package.[29] Full geometry optimization was performed at the Hartree−Fock (HF) level using the 3-21G and 6-311G basis set with the Fopt keyword. The single-point calculations were also carried out at the MP2 level with density functional theory method (B3LYP) using the 6-311G basis set.

Materials and Solvents. Zinc bilindione **1** was prepared by the similar procedure of Falk.[30] (Oxoniaporphyrinato)zinc(II) chlorides **16a**−**c** were prepared following the method of Fuhrhop.[18b] Preparation of 19-alkoxy-22*H*-bilin-1-ones **17a**−**e** was carried out by the method of Fuhrhop,[18c] which was somewhat modified by us. Amino acid esters for the spectroscopic measurements were obtained by neutralization of commercially available hydrochlorides followed by distillation just prior to use: L-Ala-OMe·HCl, L-Phe-OMe·HCl, L-Asp-$(OMe)_2$·HCl, L-Glu-$(OMe)_2$·HCl, and D-Trp-OMe·HCl were purchased from Sigma Chemical Company, L-Val-OMe·HCl, L-Leu-OMe·HCl, Gly-OMe·HCl, and L-Trp-OMe·HCl were from Nacalai Tesque Chemical Company, L-Ile-OMe·HCl was from Peptide Institute, Inc., L-Met-OMe·HCl was from Kokusan Chemical Works, and D-PhGly-OMe·HCl was from Wako Pure Chemicals Industries. Compounds (*R*)-**18** and (*S*)-**18** were purchased from Nacalai Tesque, Inc., and used without purification. Compound (*R*)-**19** was purchased from Tokyo Chemical Industries and used after distillation. Compounds (*R*)-**20**, (*S*)-**21**, and (*R*)-**22** were purchased from Aldrich Chemical Co., Inc., and used without purification. All solvents for the UV−vis, CD, and NMR measurements were of spectroscopic grade.

Zinc(II) Complex of 15a (1). This compound was reported by Falk et al. and prepared by their procedure (mp > 350 °C).[30] For **1**: ^{1}H NMR (500 MHz, $CDCl_3$) δ 0.93 (t, J = 7.6 Hz, 3H), 1.11−1.18 (m, 12H), 1.61 (s, 3H), 1.89 (s, 3H), 2.06 (s, 3H), 2.23−2.29 (m, 2H), 2.36 (q, J = 7.6 Hz, 2H), 2.49−2.60 (m, 4H), 5.60 (s, 1H), 5.82 (s, 1H), 6.64 (s, 1H); UV−vis (CH_2Cl_2, 15 °C) ϵ_{366} = 32 200, ϵ_{674} = 15 300 M^{-1} cm^{-1}; FAB MS *m*/*z* 560 ([M^+]); HR FAB MS calcd for [$C_{31}H_{36}N_4O_2{}^{64}Zn$]$^+$ 560.2130, found 560.2146.

Zn(II) Complex of 15c (2). Compound **15c** (84.0 mg, 0.150 mmol) was dispersed in a saturated ethanolic solution of zinc acetate (45 mL), followed by stirring at reflux for 0.5 h. As the temperature raised, the reaction mixture became a dark green homogeneous solution. After cooling, water (45 mL) was added, and precipitates were collected by filtration, which were dried in vacuo over silica gel. Recrystallization from ethanol afforded **2** as a dark green powder (58.0 mg, 0.0932 mmol, 62%): mp 248−250 °C (dec); ^{1}H NMR (500 MHz, DMSO-d_6) δ 1.08 (t, J = 7.9 Hz, 6H), 1.14 (t, J = 7.9 Hz, 6H), 2.01 (s, 6H), 2.39 (t, J = 7.3 Hz, 4H), 2.52−2.59 (m, 8H), 3.46 (m, 4H), 4.75 (br s, 2H, D_2O exchangeable), 5.97 (s, 2H), 6.75 (s, 1H), 9.68 (s, 1H, D_2O exchangeable); IR (KBr) 3397, 2965, 2931, 2870, 1686, 1576, 1206 cm^{-1}; UV−vis (CH_2Cl_2, 15 °C) ϵ_{358} = 39 700, ϵ_{726} = 13 600 M^{-1} cm^{-1}; FAB MS *m*/*z* 621 ([M + H]$^+$); HR FAB MS calcd for [$C_{33}H_{40}N_4O_4{}^{64}Zn$]$^+$ 620.2341, found 620.2322. Anal. Calcd for $C_{33}H_{40}N_4O_4Zn$·2.2 H_2O: C, 59.90; H, 6.76; N, 8.47. Found: C, 59.93; H, 7.28; N, 8.06.

Zn(II) Complex of 15b (3). Compound **15b** (321 mg, 0.499 mmol) was dissolved in a small amount of CH_2Cl_2 (ca. 5 mL), and to the solution was added a saturated ethanolic solution of zinc acetate (75 mL), followed by stirring at reflux for 0.5 h. After cooling, water (75 mL) was added and green solids were collected by filtration. The solid was dispersed in ethanol (50 mL), and the suspension was refluxed for 15 min. After cooling, the solid was collected by filtration, washed with a small amount of ether and then dried in vacuo to yield **3** as a dark green powder (337 mg, 0.477 mmol, 95%): mp 272−274 °C (dec); ^{1}H NMR (500 MHz, DMSO-d_6) δ 1.08−1.16 (m, 12H), 1.98 (s, 6H), 2.02 (s, 6H), 2.52−2.62 (m, 6H), 4.09 (m, 4H), 6.03 (s, 2H), 6.77 (s, 1H), 9.68 (br s, 1H, D_2O exchangeable) (six other protons seem to be masked by residual solvent protons and H_2O); IR (KBr) 3440, 2965, 2931, 2871, 1738, 1687, 1576,

(28) Riddick, J. A.; Bunger, W. B.; Sakano, T. K. *Organic Solvents*; Wiley and Sons: New York, 1986.

(29) Frisch, M. J.; Trucks, G. W.; Schlegel, H. B.; Gill, P. M. W.; Johnson, B. G.; Robb, M. A.; Cheeseman, J. R.; Keith, T.; Petersson, G. A.; Montgomery, J. A.; Raghavachari, K.; Al-Laham, M. A.; Zakrzewski, V. G.; Ortiz, J. V.; Foresman, J. B.; Cioslowski, J.; Stefanov, B. B.; Nanayakkara, A.; Challacombe, M.; Peng, C. Y.; Ayala, P. Y.; Chen, W.; Wong, M. W.; Andres, J. L.; Replogle, E. S.; Gomperts, R.; Martin, R. L.; Fox, D. J.; Binkley, J. S.; Defrees, D. J.; Baker, J.; Stewart, J. P.; Head-Gordon, M.; Gonzalez, C.; Pople, J. A. *Gaussian 94, Revision D.4*; Gaussian, Inc.: Pittsburgh, PA, 1996.

(30) Falk, H.; Schlederer, T. *Liebigs Ann. Chem.* **1979**, 1560−1570.

1245, 1204 cm^{-1}; UV−vis (CH_2Cl_2, 15 °C) $\epsilon_{360} = 36\,900$, $\epsilon_{706} = 12\,800\ M^{-1}\ cm^{-1}$; FAB MS *m/z* 705 ([M + H]$^+$); HR FAB MS calcd for [$C_{37}H_{45}N_4O_6{}^{64}Zn$]$^+$ 705.2631, found 705.2646. Anal. Calcd for $C_{37}H_{44}N_4O_6Zn\cdot 2H_2O$: C, 59.88; H, 6.52; N, 7.55. Found: C, 60.20; H, 6.11; N, 7.21.

Zn(II) Complex of 17a (4). A mixture of **17a** (115.0 mg, 0.224 mmol) and MeOH saturated with zinc acetate (45 mL) was heated at reflux for 30 min. After cooling, the reaction mixture was condensed to ca. 10 mL by evaporation, and CH_2Cl_2 (80 mL) was added. Precipitates of insoluble zinc acetate were removed by filtration, which were washed with a small amount of CH_2Cl_2 (ca. 10 mL). The washing was combined to the filtrate, washed with water (100 mL × 2), and saturated (sat.) brine (100 mL), and dried over anhydrous Na_2SO_4. The solvent was removed by evaporation, and the resultant solid was recrystallized from CH_2Cl_2−hexane to yield **4** as a dark green powder (113 mg, 0.196 mmol, 88%): mp 260−262 °C (dec); ^{1}H NMR (500 MHz, CD_2Cl_2) δ 1.118 (t, J = 7.6 Hz, 3H, CH_3CH$_2$), 1.122 (t, J = 7.6 Hz, 3H, CH_3CH$_2$), 1.14 (t, J = 7.6 Hz, 3H, 8-CH_3CH$_2$), 1.17 (t, J = 7.6 Hz, 3H, 17-CH_3CH$_2$), 1.72 (s, 3H, 18-Me), 1.75 (s, 3H, 2-Me), 2.01 (s, 3H, 7-Me), 2.07 (s, 3H, 13-Me), 2.40 (q, J = 7.6 Hz, 3-CH$_3$CH_2), 2.48−2.59 (m, 6H, 8,12,17-CH$_3$CH_2), 4.16 (s, 3H, MeO), 5.53 (s, 1H, 5-H), 6.52 (s, 1H, 10-H), 6.53 (s, 1H, 15-H); IR (KBr) 2965, 2931, 2870, 1663, 1570, 1207 cm^{-1}; UV−vis (CH_2Cl_2, 15 °C) $\epsilon_{402} = 33\,600$, $\epsilon_{780} = 17\,000\ M^{-1}\ cm^{-1}$; FAB MS *m/z* 574 ([M$^+$]); HR FAB MS calcd for [$C_{32}H_{38}N_4O_2{}^{64}Zn$]$^+$ 574.2286, found 574.2297. Anal. Calcd for $C_{32}H_{38}N_4O_2Zn$: C, 66.72; H, 6.65; N, 9.73. Found: C, 66.98; H, 6.81; N, 9.56.

Zn(II) Complex of 17c (5). To a solution of **17c** (88.0 mg, 0.154 mmol) in CH_2Cl_2 (1 mL) was added MeOH saturated with zinc acetate (35 mL), and the mixture was stirred under reflux for 1 h. After cooling, CH_2Cl_2 (40 mL) was added and washed with water (40 mL × 2) and sat. brine (40 mL). After drying over anhydrous Na_2SO_4, recrystallization of the residue from CH_2Cl_2−hexane afforded a dark green powder of **5** (72.0 mg, 0.113 mmol, 73%): mp 194−196 °C (dec); ^{1}H NMR (500 MHz, $CDCl_3$) δ 1.09−1.13 (m, 9H), 1.22 (t, J = 7.6 Hz, 3H), 1.95 (s, 3H), 2.00 (s, 3H), 2.26−2.31 (m, 1H), 2.34 (q, J = 7.6 Hz, 2H), 2.39−2.54 (m, 9H), 3.57−3.62 (m, 1H), 3.64−3.73 (m, 3H), 3.84 (br s, 1H, D_2O exchangeable), 4.04 (br s, 1H, D_2O exchangeable), 4.40 (s, 3H), 5.47 (s, 1H), 6.39 (s, 1H), 6.40 (s, 1H); IR (KBr) 3462, 2962, 2931, 2870, 1605, 1572, 1531, 1201 cm^{-1}; UV−vis (CH_2Cl_2, 15 °C) $\epsilon_{404} = 36\,500$, $\epsilon_{801} = 14\,400\ M^{-1}\ cm^{-1}$; FAB MS *m/z* 634 ([M$^+$]); HR FAB MS calcd for [$C_{34}H_{42}N_4O_4{}^{64}Zn$]$^+$ 634.2498, found 634.2471. Anal. Calcd for $C_{34}H_{42}N_4O_4Zn\cdot 1.5H_2O$: C, 61.58; H, 6.84; N, 8.45. Found: C, 61.56; H, 6.55; N, 8.20.

Zn(II) Complex of 17b (6). A mixture of **17b** (127 mg, 0.193 mmol) and MeOH saturated with zinc acetate (35 mL) was heated at reflux for 1 h. After cooling, CH_2Cl_2 (60 mL) was added and washed with water (60 mL × 3) and sat. brine (60 mL). Drying over anhydrous Na_2SO_4 followed by recrystallization of the residue from CH_2Cl_2−hexane afforded a dark green powder of **6** (78.0 mg, 0.108 mmol, 56%): mp 203−204.5 °C (dec); ^{1}H NMR (500 MHz, $CDCl_3$) δ 1.11 (t, J = 7.6 Hz, 3H), 1.13 (t, J = 7.6 Hz, 3H), 1.15 (t, J = 7.6 Hz, 3H), 1.20 (t, J = 7.6 Hz, 3H), 1.98 (s, 3H), 2.006 (s, 3H), 2.012 (s, 3H), 2.04 (s, 3H), 2.40 (q, J = 7.6 Hz, 2H), 2.46−2.59 (m, 10H), 3.99−4.05 (m, 2H), 4.09−4.12 (2H, m), 4.26 (s, 3H), 5.49 (s, 1H), 6.44 (s, 1H), 6.49 (s, 1H); IR (KBr) 2964, 2930, 2873, 1740, 1655, 1572, 1244, 1206 cm^{-1}; UV−vis (CH_2Cl_2, 15 °C) $\epsilon_{408} = 35\,100$, $\epsilon_{794} = 15\,300\ M^{-1}\ cm^{-1}$; FAB MS *m/z* 718 (M$^+$); HR FAB MS calcd for [$C_{38}H_{46}N_4O_6{}^{64}Zn$]$^+$ 718.2709, found 718.2740. Anal. Calcd for $C_{38}H_{46}N_4O_6Zn$: C, 63.37; H, 6.44; N, 7.78. Found: C, 62.99; H, 6.49; N, 7.87.

Zn(II) Complex of 17e (7). A mixture of **17e** (80.0 mg, 0.141 mmol) was dissolved in CH_2Cl_2 (1 mL). To the solution was added MeOH saturated with zinc acetate (25 mL), and the mixture was stirred under reflux for 1 h. After cooling, the solvent was removed by evaporation. To the residue was added CH_2Cl_2 (40 mL) and washed with water (40 mL × 2) and sat. brine (40 mL). After drying over anhydrous Na_2SO_4, recrystallization from of the residue CH_2Cl_2−hexane afforded a dark green powder of **7** (65.6 mg, 0.104 mmol, 74%): mp 202−204 °C (dec); ^{1}H NMR (500 MHz, $CDCl_3$) δ 0.86−0.89 (m, 6H), 1.11 (t, J = 7.6 Hz, 3H), 1.12−1.15 (m, 6H), 1.17 (t, J = 7.6 Hz, 3H), 1.36−1.49 (m, 4H), 2.00 (s, 3H), 2.05 (s, 3H), 2.09 (t, J = 7.6 Hz, 2H), 2.17 (t, J = 7.6 Hz, 2H), 2.39 (q, J = 7.6 Hz, 2H), 2.43−2.56 (m, 6H), 4.20 (s, 3H), 5.48 (s, 1H), 6.47 (s, 1H), 6.48 (s, 1H); IR (KBr) 2959, 2926, 2867, 1658, 1575, 1204 cm^{-1}; UV−vis (CH_2Cl_2, 15 °C) $\epsilon_{402} = 35\,000$, $\epsilon_{786} = 17\,200\ M^{-1}\ cm^{-1}$; FAB MS *m/z* 630 ([M$^+$]); HR FAB MS calcd for [$C_{36}H_{46}N_4O_2{}^{64}Zn$]$^+$ 630.2912, found 630.2928. Anal. Calcd for $C_{36}H_{46}N_4O_2Zn$: C, 68.40; H, 7.33; N, 8.86. Found: C, 68.09; H, 7.39; N, 8.67.

Zn(II) Complex of 17d (8). This compound was prepared by a procedure similar to that employed for **4** using **17d** (115.0 mg, 0.224 mmol) dissolved in a small amount of CH_2Cl_2 and 2-propanol saturated with zinc acetate (75 mL). The reaction mixture was treated by the analogous procedure to that used for **4**, and the crude product was recrystallized from CH_2Cl_2−hexane to yield **8** as a dark green crystal (130 mg, 0.215 mmol, 85%): mp 222−224 °C (dec); ^{1}H NMR (500 MHz, $CDCl_3$) δ 1.10−1.17 (m, 12H), 1.20 (d, J = 5.9 Hz, 3H), 1.34 (d, J = 5.9 Hz, 3H), 1.71 (s, 3H), 1.76 (s, 3H), 2.02 (s, 3H), 2.07 (s, 3H), 2.38 (q, J = 7.8 Hz, 2H), 2.40−2.56 (m, 6H), 5.46 (spt, J = 5.9 Hz, 1H), 5.54 (s, 1H), 6.49 (s, 1H), 6.50 (s, 1H); IR (KBr) 2965, 2930, 2870, 1663, 1574, 1207 cm^{-1}; UV−vis (CH_2Cl_2, 15 °C) $\epsilon_{401} = 34\,700$, $\epsilon_{778} = 17\,200\ M^{-1}\ cm^{-1}$; FAB MS *m/z* 602 ([M$^+$]); HR FAB MS calcd for [$C_{34}H_{42}N_4O_2{}^{64}Zn$]$^+$ 602.2599, found 602.2573. Anal. Calcd for $C_{34}H_{42}N_4O_2Zn$: C, 67.60; H, 7.01; N, 9.27. Found: C, 67.30; H, 7.11; N, 8.85.

Methyl (4-Acetyl-2-methoxycarbonyl-5-methyl-1*H*-pyrrol-3-yl)acetate (9b). To a mixture of 1,3-acetonedicarboxylic acid (92.0 g, 0.528 mol) and concentrated HCl (2.0 mL) was added dropwise amyl nitrite (67.9 g, 0.580 mol) over 3 h below 5 °C. After 12 h of stirring at room temperature, acetic acid (550 mL), acetylacetone (58.0 g, 0.580 mol), and sodium acetate (52.5 g, 0.640 mol) were added to the mixture, followed by zinc powder (104 g, 1.59 mol) in portions with vigorous stirring. The reaction was exothermic, and the temperature in the flask was kept between 70 and 90 °C during the addition of zinc. The mixture was then heated at 100 °C for 3 h. The hot mixture was poured into ice−water, and the resultant suspension was allowed to stand for a few hours. The zinc dusts were removed by decantation, and the suspension was extracted with CH_2Cl_2 (300 mL × 3). The organic layer was washed with water (500 mL × 2) and sat. brine (500 mL), followed by drying over anhydrous $MgSO_4$. After removal of the solvent, the residue was recrystallized from $CHCl_3$−hexane to yield **9b** as a pale yellow solid (66.8 g, 0.264 mol, 50%): mp 138−140 °C; ^{1}H NMR (270 MHz, $CDCl_3$) δ 2.42 (s, 3H), 2.54 (s, 3H), 3.73 (s, 3H), 3.85 (s, 3H), 4.20 (s, 2H), 9.25 (br s, 1H); IR (KBr) 3286, 2956, 1734, 1673, 1646 cm^{-1}; EI MS (relative intensity) *m/z* 253 (M$^+$, 39), 221 (100), 193 (59), 162 (81). Anal. Calcd for $C_{12}H_{15}NO_5$: C, 56.91; H, 5.97; N, 5.53. Found: C, 56.66; H, 6.03; N, 5.32.

Ethyl 4-Acetyl-5-methyl-3-propyl-1*H*-pyrrole-2-carboxylate (9c). To a solution of ethyl 3-oxohexanoate (25.2 g, 0.159 mol) in acetic acid (75 mL) was added dropwise below 5 °C a solution of sodium nitrite (13.2 g, 0.191 mol) in H_2O (25 mL). The mixture was stirred overnight at room temperature, followed by adding acetylacetone (17.5 g, 0.175 mol) and sodium acetate (17.0 g, 0.207 mol) and then heating at 60 °C. Zinc powder (22.9 g, 0.350 mol) was added portionwise so as to keep the temperature at 90 °C. After completion of addition of zinc, the mixture was heated with vigorous stirring at 100 °C for 2.5 h. The hot mixture was poured into 500 g of ice, and the solids that precipitated were extracted with CH_2Cl_2 (200 mL × 3). The organic phase was washed with water (300 mL × 2) and sat. brine (300 mL) and dried over anhydrous $MgSO_4$. Evaporation afforded the solid residue, which was recrystallized from hexanes−ethyl acetate to yield **9c** as an ivory crystal (23.1 g, 0.0975 mol, 61%): mp 107−109 °C; ^{1}H NMR (270 MHz, $CDCl_3$) δ 0.98 (t, J = 7.3 Hz, 3H), 1.38 (t, J = 7.3 Hz, 3H), 1.57 (sextet, J = 7.3 Hz, 2H), 2.46 (s, 3H), 2.53 (s, 3H), 3.03 (t, J = 7.3 Hz, 2H), 4.34 (q, J = 7.3 Hz, 2H), 9.39 (br s, 1H); IR (KBr) 3178, 3111, 3054, 2983, 2957, 2870, 1689, 1629, 1284 cm^{-1}; EI MS (rel intensity) *m/z* 237 (M$^+$, 39), 222

(39), 208 (25), 190 (30), 176 (100). Anal. Calcd for $C_{13}H_{19}NO_3$: C, 65.80; H, 8.07; N, 5.90. Found: C, 65.61; H, 8.19; N, 5.67.

Methyl 4-Ethyl-3-(2-hydroxyethyl)-5-methyl-1*H*-pyrrole-2-carboxylate (10b). A mixture of **9b** (29.7 g, 0.117 mol) and $NaBH_4$ (17.5 g, 0.463 mol) in THF (360 mL) was cooled to 0 °C and then BF_3·Et_2O (101 g, 0.712 mol) was added dropwise over 2 h so as to maintain the reaction mixture at 0 °C. After 4 h of stirring, water (50 mL) and 1 M HCl (20 mL) were added while cooled in an ice bath, followed by neutralization with sat. $NaHCO_3$. The THF was removed by evaporation, and the aqueous mixture was extracted with CH_2Cl_2 (350 mL × 3). The organic layer was washed with water (500 mL × 2) and sat. brine (500 mL), followed by drying over anhydrous $MgSO_4$. Evaporation followed by drying in vacuo afforded **10b** as an ivory solid (20.6 g, 0.0975 mol, 84%). The product was pure on the basis of the ^{1}H NMR spectra, and it was used in the following reaction without further purification: mp 110−112 °C; ^{1}H NMR (270 MHz, $CDCl_3$) δ 1.06 (t, J = 7.3 Hz, 3H), 2.21 (s, 3H), 2.40 (q, J = 7.3 Hz, 2H), 3.01 (t, J = 6.7 Hz, 2H), 3.78 (t, J = 6.7 Hz, 2H), 3.81 (s, 3H), 8.96 (br s, 1H); IR (KBr) 3331, 2961, 2928, 2869, 1680, 1271 cm^{-1}; EI MS (rel intensity) m/z 211 (M^+, 67), 180 (100), 148 (59). Anal. Calcd for $C_{11}H_{17}NO_3$: C, 62.53; H, 8.11; N, 6.63. Found: C, 62.14; H, 8.31; N, 6.50.

Ethyl 4-Ethyl-5-methyl-3-propyl-1*H*-pyrrole-2-carboxylate (10c). A mixture of **9c** (22.1 g, 0.0931 mol) and $NaBH_4$ (8.88 g, 0.235 mol) in THF (200 mL) was cooled below 0 °C. To the mixture was added dropwise BF_3·Et_2O (46.2 g, 0.325 mol) so that the temperature of the solution could be kept at 0 °C. After the addition of BF_3·Et_2O was completed, the mixture was stirred for 1 h at room temperature. Water (50 mL) and concentrated HCl (20 mL) were carefully added while cooled in an ice bath with stirring, and then the mixture was neutralized with sat. $NaHCO_3$, followed by removal of the THF by evaporation. The residual water layer was extracted with CH_2Cl_2 (200 mL × 2). The organic phase was washed with water (200 mL × 2) and sat. brine (200 mL) and dried over anhydrous $MgSO_4$. The solvent was removed and the residue was dried in vacuo to afford **10c** (18.6 g, 0.0834 mol, 90%), which was used in the next step without further purification: mp 98−99 °C; ^{1}H NMR (270 MHz, $CDCl_3$) δ 0.96 (t, J = 7.3 Hz, 3H), 1.06 (t, J = 7.3 Hz, 3H), 1.34 (t, J = 7.3 Hz, 3H), 1.54 (sextet, J = 7.3 Hz, 2H), 2.21 (s, 3H), 2.38 (q, J = 7.3 Hz, 2H), 2.66 (t, J = 7.3 Hz, 2H), 4.28 (q, J = 7.3 Hz, 2H), 8.70 (br s, 1H); IR (KBr) 3304, 2960, 2927, 2866, 1672, 1272 cm^{-1}; EI MS (rel intensity) m/z 223 (M^+, 85), 208 (23), 194 (93), 176 (22), 162 (55), 148 (100). Anal. Calcd for $C_{13}H_{21}NO_2$: C, 69.92; H, 9.48; N, 6.27. Found: C, 70.07; H, 9.74; N, 6.12.

2-(3-Ethyl-2-methyl-1*H*-pyrrol-4-yl)ethanol (11b). A solution of **10b** (10.6 g, 0.0502 mol) and NaOH (6.02 g, 0.151 mol) in 3:1 (v/v) EtOH/H_2O (120 mL) was heated at reflux for 3 h. After cooling to room temperature, the solution was condensed to ca. 30 mL by evaporation. Acidification to pH 3 with concentrated HCl in an ice−water bath afforded pale pink precipitates, which were collected by filtration and then dried in vacuo. The solid was dissolved in ethanolamine (100 mL) and heated at reflux for 2.5 h. After cooling, the solution was poured to water (500 mL) followed by extraction with CH_2Cl_2 (150 mL × 3). The organic layer was washed with water (300 mL × 2) and sat. brine (300 mL) and dried over anhydrous $MgSO_4$. The solvent was removed by evaporation to yield **11b** (6.61 g, 0.0431 mol, 86%) as a dark red oil. The product was quite unstable, so it was used in the following reaction without purification: ^{1}H NMR (500 MHz, $CDCl_3$) δ 1.08 (t, J = 7.6 Hz, 3H), 2.18 (s, 3H), 2.40 (q, J = 7.6 Hz, 2H), 2.70 (t, J = 6.7 Hz, 2H), 3.74 (t, J = 6.7 Hz, 2H), 6.47 (d, J = 2.1 Hz, 1H), 7.68 (br s, 1H) (the OH proton was not observed); IR (KBr) 3367, 2960, 2924, 2871 cm^{-1}; EI MS (rel intensity) m/z 153 (M^+, 45), 122 (100); HR EI MS calcd for $[C_9H_{15}NO]^+$ 153.1153, found 153.1158.

3-Ethyl-2-methyl-4-propyl-1*H*-pyrrole (11c). To a solution of **10c** (17.5 g, 0.0784 mol) in ethanol (85 mL) was added a solution of NaOH (10.2 g, 0.255 mol) in water (30 mL). The mixture was heated at reflux for 3.5 h. After cooling, the mixture was condensed to ca. 30 mL and acidified to pH 3 with concentrated HCl. The pale pink solid was precipitated, which was separated by filtration. The filtrate was separated into two phases, from which the organic layer was taken up with ether (50 mL × 2). The solids were dried over P_2O_5 in vacuo and then dissolved in ethanolamine (100 mL) followed by reflux for 30 min. After cooling, the solution was poured into water (500 mL) and extracted with ether several times until the organic phase became colorless. The ether layer was combined with the former ether extract, washed with H_2O (250 mL × 2) and sat. brine (250 mL), and dried over anhydrous $MgSO_4$. After removal of the solvent, the residue was distilled at the reduced pressure to afford **11c** as a colorless oil (7.05 g, 0.0466 mol, 59%): bp 91−93 °C at 1 mmHg; ^{1}H NMR (270 MHz, $CDCl_3$) δ 0.98 (t, J = 7.3 Hz, 3H), 1.08 (t, J = 7.3 Hz, 3H), 1.58 (sextet, J = 7.3 Hz, 2H), 2.17 (s, 3H), 2.35−2.43 (m, 4H), 6.37 (d, J = 2.4 Hz, 2H), 7.49 (br s, 1H); IR (CCl_4) 3487, 2961, 2928, 2869 cm^{-1}; EI MS (rel intensity) m/z 151 (M^+, 43), 136 (28), 122 (100); HR EI MS calcd for $[C_{10}H_{17}N]^+$ 151.1361, found 151.1365.

2-(4-Ethyl-2,5-dihydro-5-methyl-2-oxo-1*H*-pyrrol-3-yl)-ethanol (12b). To a solution of **11b** (6.61 g, 0.0431 mol) in a solvent mixture of MeOH and water (3:1, v/v, 55 mL) was added dropwise 30% H_2O_2 (5.36 g, 0.0437 mol) at 50 °C. The mixture was stirred for 2.5 h at the same temperature and then heated at reflux for 1.5 h. After cooling, a solution of K_2CO_3 (2.35 g, 0.0170 mol) in 25 mL of water was added, and the resultant mixture was stirred overnight. The mixture was condensed to ca. 15 mL by evaporation and neutralized with concentrated HCl, followed by extraction with CH_2Cl_2 (100 mL × 3). The organic layer was dried over anhydrous $MgSO_4$. The solvent was removed by evaporation, and the residue was purified by silica gel column chromatography (20:1 CH_2Cl_2−MeOH, v/v, as eluent). Crystallization was induced by scratching the product obtained as an oil on the flask to yield **12b** (3.91 g, 0.0231 mol, 54%) as an ivory solid: mp 90−92 °C; ^{1}H NMR (270 MHz, $CDCl_3$) δ 1.09 (t, J = 7.3 Hz, 3H), 1.29 (d, J = 6.7 Hz, 3H), 2.17−2.30 (m, 1H, CH_3CHH), 2.40−2.51 (m, 1H, CH_3CHH), 2.54 (t, J = 5.5 Hz, 2H), 3.73 (q, J = 5.5 Hz, 2H), 4.15 (q, J = 6.7 Hz, 1H), 4.35 (t, J = 5.5 Hz, 1H), 7.33 (br s, 1H); IR (KBr) 3397, 3359, 3249, 2972, 2935, 2874, 1681 cm^{-1}; EI MS (rel intensity) m/z 169 (M^+, 18), 151 (55), 139 (100). Anal. Calcd for $C_9H_{15}NO_2$: C, 63.88; H, 8.93; N, 8.28. Found: C, 63.50; H, 9.17; N, 8.07.

2,5-Dihydro-4-ethyl-5-methyl-2-oxo-3-propyl-1*H*-pyrrole (12c). To a solution of **11c** (6.56 g, 0.0434 mol) in a solvent mixture of MeOH and water (3:1, v/v, 50 mL) was added dropwise 30% H_2O_2 (6.56 g, 0.0579 mol) at 55 °C. The mixture was stirred for 2 h at the same temperature and then heated at reflux for 2 h. After cooling, K_2CO_3 (2.99 g, 0.0216 mol) in 20 mL of water was added, followed by stirring overnight at room temperature. The mixture was neutralized with 1 M HCl, and the MeOH was removed by evaporation. The residual solution was extracted with CH_2Cl_2 (50 mL × 3), and the organic layer was washed with water (50 mL × 2) and sat. brine (50 mL), followed by drying over anhydrous $MgSO_4$. The solvent was removed, and the residue was purified by distillation at reduced pressure to afford **12c** (5.68 g, 0.0340 mol, 78%): bp 91−93 °C at 1 mmHg; ^{1}H NMR (270 MHz, $CDCl_3$) δ 0.92 (t, J = 7.3 Hz, 3H), 1.09 (t, J = 7.3 Hz, 3H), 1.26 (d, J = 6.7 Hz, 3H), 1.51 (sextet, J = 7.3 Hz, 3H), 2.14−2.29 (m, 3H, CH_3CHH), 2.42−2.56 (m, 1H, CH_3CHH), 4.07 (q, J = 6.7 Hz, 1H), 6.79 (br s, 1H); IR (CCl_4) 3213, 2969, 2935, 2873, 1689 cm^{-1}; EI MS (rel intensity) m/z 167 (M^+, 66), 152 (32), 138 (100); HR EI MS calcd for $[C_{10}H_{17}NO]^+$ 167.1310, found 167.1304.

2-(5-Bromomethylene-4-ethyl-2,5-dihydro-2-oxo-1*H*-pyrrol-3-yl)ethyl Acetate (13b). To a stirred solution of **12b** (18.6 g, 0.110 mol) in ethyl acetate (200 mL) was added dropwise Br_2 (35.6 g, 0.222 mol) at 55 °C. The mixture was stirred at reflux for 15 min. After cooling, the solution was washed with sat. $NaHCO_3$ (150 mL × 3), water (150 mL), and sat. brine (150 mL). During washing the solution, heavy precipitate formed, which was removed by filtration. The

organic layer was dried over anhydrous $MgSO_4$, reduced to 50 mL by evaporation, and then cooled to −20 °C. The light brown solid was precipitated, which was filtered to yield **13b** (13.1 g, 0.0455 mol). The filtrate was evaporated to dryness, followed by purification of the residue by silica gel chromatography (5:1 benzene−acetone, v/v, as eluent) to afford another crop of **13b** (5.97 g, 0.0207 mol): total yield 60%; mp 113.7−114.2 °C; ^{1}H NMR (270 MHz, $CDCl_3$) δ 1.18 (t, J = 7.9 Hz, 3H), 2.03 (s, 3H), 2.45 (q, J = 7.9 Hz, 2H), 2.65 (t, J = 6.7 Hz, 2H), 4.22 (t, J = 6.7 Hz, 2H), 5.98 (s, 1H), 7.37 (br s, 1H); IR (KBr) 3161, 3102, 2969, 2934, 2875, 1740, 1705, 1641, 1241 cm^{-1}; EI MS (rel intensity) m/z 289 (5, $M^+ + 2$), 287(5, M^+), 246 (19), 244 (19), 229 (99), 227 (100), 202 (8), 200 (8). Anal. Calcd for $C_{11}H_{14}NO_3Br$: C, 45.85; H, 4.90; N, 4.86. Found: C, 45.47; H, 4.85; N, 4.59.

5-Bromomethylene-4-ethyl-2,5-dihydro-2-oxo-3-propyl-1*H*-pyrrole (13c). To a stirred solution of **12c** (5.35 g, 0.0320 mol) in ethyl acetate (45 mL) was added Br_2 (3.3 mL, 0.064 mol) at 55 °C over 1 h. After the completion of the addition, the mixture was heated at reflux for 15 min. After cooling, the solution was washed with sat. $NaHCO_3$ (100 mL × 3), water (100 mL), and sat. brine (100 mL), and then was dried over $MgSO_4$. The solvent was evaporated to afford precipitates, which were separated by filtration and washed with a small amount of cold ether. The filtrate and washings were combined and evaporated. To the residue was added a small amount of hexane, followed by standing overnight at −20 °C to afford precipitates. This procedure was repeated until further precipitations were not obtained. All the precipitates were combined and dried in vacuo to yield **13c** (5.96 g, 0.0244 mol, 76%), which was used in the next step without further purification: mp 89−91 °C; ^{1}H NMR (270 MHz, $CDCl_3$) δ 0.94 (t, J = 7.3 Hz, 3H), 1.16 (t, J = 7.3 Hz, 3H), 1.54 (sextet, J = 7.3 Hz, 2H), 2.27 (t, J = 7.3 Hz, 2H), 2.42 (q, J = 7.3 Hz, 2H), 5.91 (s, 1H), 7.24 (br s, 1H); IR (KBr) 3166, 3104, 2958, 2935, 2872, 1704, 1691, 1641 cm^{-1}; EI MS (rel intensity) m/z 245 (99, $M^+ + 2$), 243(100, M^+), 230 (36), 228 (39), 216 (65), 214 (64), 164 (73), 136 (89), 135 (76); HR EI MS calcd for $[C_{10}H_{14}NOBr]^+$ 243.0259, found 243.0268.

2-[3,8-Diethyl-7,9-dimethyl-1-oxo-1,10-dihydrodipyrrin-2-yl]ethyl Acetate (14b). A mixture of 4-ethyl-3,5-dimethyl-1*H*-pyrrole-2-carboxylic acid (2.61 g, 15.6 mmol) and **13b** (2.07 g, 7.18 mmol) in MeOH (15 mL) was heated at reflux for 1 h. After cooling, the yellow precipitates were collected by filtration and dissolved in a small amount of CH_2Cl_2. Addition of MeOH with stirring afforded a yellow solid, and the suspension was cooled to −20 °C. The solid was filtered and dried in vacuo to yield **14b** (1.42 g, 4.31 mmol, 60%) which was used in the next step without further purification: mp 184−185 °C (dec); ^{1}H NMR (500 MHz, $CDCl_3$) δ 1.08 (t, J = 7.9 Hz, 3H), 1.23 (t, J = 7.9 Hz, 3H), 2.02 (3H, s), 2.14 (3H, s), 2.37 (3H, s), 2.41 (q, J = 7.9 Hz, 2H), 2.60 (q, J = 7.9 Hz, 2H), 2.74 (t, J = 6.9 Hz, 2H), 4.20 (t, J = 6.9 Hz, 2H), 6.21 (s, 1H), 10.3 (br s, 1H), 11.3 (br s, 1H); IR (KBr) 3342, 2966, 2932, 2872, 1742, 1673, 1637, 1239 cm^{-1}; EI MS (rel intensity) m/z 330 (M^+, 100), 270 (88). Anal. Calcd for $C_{19}H_{26}N_2O_3$: C, 69.06; H, 7.93; N, 8.48. Found: C, 68.68; H, 8.10; N, 8.32.

3,8-Diethyl-7,9-dimethyl-1-oxo-2-propyl-1,10-dihydrodipyrrin (14c). A mixture of 3-ethyl-2,4-dimethyl-1*H*-pyrrole (1.49 g, 0.0121 mol) and **13c** (2.44 g, 0.0100 mol) in MeOH (20 mL) was heated at reflux under Ar for 2 h. After cooling, the mixture was allowed to stand overnight at −20 °C to afford yellow precipitates, which were separated by filtration. Washing the precipitates with CH_2Cl_2−MeOH (1:1, v/v, 75 mL) afforded **14c** (1.68 g, 5.85 mmol, 59%), which was used in the next step without further purification: mp 211−213 °C (dec); ^{1}H NMR (500 MHz, $CDCl_3$) δ 0.94 (t, J = 7.3 Hz, 3H), 1.08 (t, J = 7.3 Hz, 3H), 1.20 (t, J = 7.3 Hz, 3H), 1.56 (sextet, J = 7.3 Hz, 2H), 2.14 (3H, s), 2.35 (t, J = 7.3 Hz, 2H), 2.40 (3H, s), 2.41−2.44 (m, 2H), 2.56 (q, J = 7.3 Hz, 2H), 6.14 (s, 1H), 10.3 (br s, 1H), 11.3 (br s, 1H); IR (KBr) 3351, 2961, 2929, 2869, 1669, 1635, 1245 cm^{-1}; EI MS (rel intensity) m/z 286 (M^+, 100), 257 (73), 241 (44), 212 (21). Anal. Calcd for $C_{18}H_{26}N_2O$: C, 75.48; H, 9.15; N, 9.78. Found: C, 75.06; H, 9.46; N, 9.65.

2,18-Bis(2-acetoxyethyl)-7,13-dimethyl-3,8,12,17-tetraethyl-1,19,21,24-tetrahydro-1,19-bilindione (15b). To a refluxed solution of *p*-chloranil (3.07 g, 12.5 mmol) in CH_2Cl_2 (300 mL) was added dropwise a solution of **14b** (1.65 g, 5.00 mmol) in CH_2Cl_2 (200 mL) over an hour, followed by addition of formic acid (30 mL). The mixture was stirred under reflux for 30 h and then condensed to ca. 300 mL, followed by stirring for additional 12 h. After cooling, the mixture was allowed to stand overnight at −20 °C to afford brownish green precipitates which were removed by filtration. The bluish green filtrate was neutralized with sat. Na_2CO_3, followed by extraction with $CHCl_3$ (200 mL × 3). The organic phase was combined, washed with water (300 mL × 2) and sat. brine (300 mL), and dried over anhydrous $MgSO_4$. The solvent was removed by evaporation to afford a dark blue residue, which was purified by silica gel column chromatography (40:1 $CHCl_3$−MeOH, v/v, as eluent). Recrystallization from $CHCl_3$−MeOH afforded a dark blue crystal of **15b** (1.15 g, 1.79 mmol, 72%): mp 214−216 °C; ^{1}H NMR (500 MHz, $CDCl_3$) δ 1.16 (t, J = 7.9 Hz, 6H), 1.25 (t, J = 7.9 Hz, 6H), 2.03 (s, 6H), 2.06 (s, 6H), 2.54 (q, J = 7.9 Hz, 4H), 2.57 (q, J = 7.9 Hz, 4H), 2.61 (t, J = 7.3 Hz, 4H), 4.16 (t, J = 7.3 Hz, 4H), 5.92 (s, 2H), 6.61 (s, 1H); IR (KBr) 3450, 2967, 2932, 2871, 1736, 1689, 1591, 1244 cm^{-1}; EI MS (rel intensity) m/z 642 (M^+, 100), 582 (27), 522 (6); HR FAB MS calcd for $[C_{37}H_{46}N_4O_6]^+$ 642.3417, found 642.3444. Anal. Calcd for $C_{37}H_{46}N_4O_6$: C, 69.14; H, 7.21; N, 8.72. Found: C, 68.78; H, 7.28; N, 8.38.

3,8,12,17-Tetraethyl-1,19,21,24-tetrahydro-2,18-bis(2-hydroxyethyl)-7,13-dimethyl-1,19-bilindione (15c). A mixture of **15b** (336 mg, 0.523 mmol), 5% HCl (15 mL) and acetone (15 mL) was boiled for 2.5 h. After cooling, 1.6 M NaOH (ca. 20 mL) was added to the reaction mixture, and the solution was acidified with acetic acid to pH 4, followed by neutralization with sat. $NaHCO_3$. Extraction with $CHCl_3$ (50 mL × 3) was carried out, and the organic phase was washed with sat. $NaHCO_3$ (50 mL), water (50 mL), and sat. brine (50 mL), and dried over anhydrous $MgSO_4$. After evaporation of the $CHCl_3$, the residue was purified by silica gel column chromatography (20:1 $CHCl_3$−MeOH, v/v, as eluent) to yield **15c** (222 mg, 0.397 mmol, 76%): mp 239−241 °C (dec); ^{1}H NMR (500 MHz, $CDCl_3$) δ 1.15 (t, J = 7.3 Hz, 6H), 1.23 (t, J = 7.9 Hz, 6H), 2.02 (s, 6H), 2.48−2.57 (m, 12H), 3.74 (t, J = 5.5 Hz, 4H), 5.86 (s, 2H), 6.54 (s, 1H) (NH and OH protons were not observed because of rapid proton exchanges); IR (KBr) 3397, 3368, 3248, 2963, 2929, 2870, 1688, 1588, 1214 cm^{-1}; HR FAB MS calcd for $[C_{33}H_{42}N_4O_4]^+$ 558.3206, found 558.3231. Anal. Calcd for $C_{33}H_{42}N_4O_4 + CH_3OH$: C, 69.13; H, 7.21; N, 8.72. Found: C, 68.78; H, 7.28; N, 8.38.

3,8,12,17-Tetraethyl-7,13-dimethyl-2,18-dipropyl-1,19,21,24-tetrahydro-1,19-bilindione (15d). To a refluxed solution of *p*-chloranil (2.46 g, 10.0 mmol) in CH_2Cl_2 (250 mL) was added dropwise a solution of **14c** (1.15 g, 4.00 mmol) in CH_2Cl_2 (300 mL) over an hour, and then formic acid (25 mL) was added at a time. The color of the solution was initially dark yellow and changed to dark bluish green as the reaction proceeded. The mixture was heated at reflux for 24 h and condensed to 150 mL by distillation, followed by reflux for additional 12 h. Cooling to −20 °C followed by standing overnight afforded heavy precipitates, which were filtered off. The filtrate was neutralized with sat. Na_2CO_3. The organic phase was separated, washed with 1 M NaOH (300 mL × 3), water (500 mL × 3), and sat. brine (500 mL × 3), and dried over $MgSO_4$. Evaporation of the organic solution followed by recrystallization from CH_2Cl_2−MeOH yielded **15d** as a dark blue crystal (614 mg, 1.11 mmol, 55%): mp 238−240 °C (dec); ^{1}H NMR (500 MHz, $CDCl_3$) δ 0.94 (t, J = 7.3 Hz, 6H), 1.17 (t, J = 7.3 Hz, 6H), 1.23 (t, J = 7.3 Hz, 6H), 1.51 (sextet, J = 7.3 Hz, 6H), 2.07 (s, 6H), 2.23 (t, J = 7.3 Hz, 4H), 2.48−2.63 (m, 8H), 5.91 (s, 2H), 6.64 (s, 1H) (NH protons were not observed because of rapid proton exchanges); IR (KBr) 2963, 2929, 2868, 1698, 1680, 1591, 1214 cm^{-1}; HR FAB MS calcd for $[C_{35}H_{46}N_4O_2]^+$ 554.3621, found 554.3644. Anal. Calcd for $C_{35}H_{46}N_4O_2$: C, 75.78; H, 8.36; N, 10.10. Found: C, 75.62; H, 8.59; N, 10.13.

(2,8,13,17-Tetraethyl-3,7,12,18-tetramethyl-5-oxoniaporphyrinato)zinc(II) Chloride (16a). A mixture of **15a** (1.20 g, 2.41 mmol), acetic anhydride (45 mL), ethanol saturated with zinc acetate (45 mL), and $CHCl_3$ (250 mL) was boiled for 0.5 h in an oil bath with a temperature of 80 °C. After cooling, the solvent was removed by evaporation, and CH_2Cl_2 (250 mL) was added to the residue, followed by washing with water (150 mL × 3), 10% NH_4Cl (150 mL × 3), and sat. brine (200 mL). After the extracts were dried over anhydrous $MgSO_4$, a dark blue solid was obtained by evaporating the solvent. Purification by silica gel column chromatography (20:1 CH_2Cl_2−MeOH, v/v, as eluent) followed by recrystallization from CH_2Cl_2−hexane yielded a dark blue crystal of **16a** (1.14 g, 1.96 mmol, 81%): mp > 250 °C (dec); ^{1}H NMR (500 MHz, $CDCl_3$) δ 1.61 (t, J = 7.9 Hz, 6H), 1.64 (t, J = 7.9 Hz, 6H), 3.00 (s, 6H), 3.06 (s, 6H), 3.48−3.58 (m, 8H), 9.19 (s, 2H), 9.27 (s, 2H); IR (KBr) 2968, 2929, 2870, 1546, 1210 cm^{-1}; FAB MS m/z 543 ([M − Cl]$^+$); HR FAB MS calcd for $[C_{31}H_{35}N_4O^{64}Zn]^+$ 543.2102, found 543.2080. Anal. Calcd for $C_{31}H_{35}N_4OZnCl$: C, 64.14; H, 6.08; N, 9.65. Found: C, 64.31; H, 6.11; N, 9.76.

[3,7-Bis(2-acetoxyethyl)-2,8,13,17-tetraethyl-12,18-dimethyl-5-oxoniaporphyrinato]zinc(II) Chloride (16b). A mixture of **15b** (324 mg, 0.504 mmol), acetic anhydride (10 mL), ethanol saturated with zinc acetate (10 mL), and $CHCl_3$ (50 mL) was boiled for 0.5 h in an oil bath with a temperature of 80 °C. After cooling, the solvent was removed by evaporation, and to the resultant mixture was added CH_2Cl_2 (75 mL). The mixture was washed with water (50 mL × 3), 10% NH_4Cl (60 mL × 3), and sat. brine (50 mL), and then dried over anhydrous $MgSO_4$, followed by removal of the solvent. Purification of the residue by silica gel column chromatography (40:1 CH_2Cl_2−MeOH, v/v, as eluent) followed by recrystallization from CH_2Cl_2-hexane yielded a dark blue crystal of **16b** (0.248 mg, 0.343 mmol, 68%): mp 216−219 °C (dec); ^{1}H NMR (500 MHz, $CDCl_3$) δ 1.62 (t, J = 7.9 Hz, 6H), 1.71 (t, J = 7.9 Hz, 6H), 2.03 (s, 6H), 3.07 (s, 6H), 3.49−3.64 (m, 8H), 3.75−3.81 (m, 2H), 3.83−3.89 (m, 2H), 4.71−4.76 (m, 2H), 4.78−4.83 (m, 2H), 9.27 (s, 2H), 9.30 (s, 1H); IR (KBr) 2967, 2932, 2873, 1740, 1546, 1243 cm^{-1}; FAB MS m/z 687 ([M − Cl]$^+$); HR FAB MS calcd for $[C_{37}H_{43}N_4O_5{}^{64}Zn]^+$ 687.2525, found 687.2530. Anal. Calcd for $C_{37}H_{43}N_4O_5ZnCl$: C, 61.33; H, 5.98; N, 7.73. Found: C, 61.26; H, 6.07; N, 7.75.

(2,8,13,17-Tetraethyl-12,18-dimethyl-3,7-dipropyl-5-oxoniaporphyrinato)zinc(II) Chloride (16c). A mixture of **15d** (277 mg, 0.499 mmol), acetic anhydride (10 mL), ethanol saturated with zinc acetate (10 mL), and $CHCl_3$ (50 mL) was boiled for 2 days in an oil bath with a temperature of 90 °C. After cooling, the solvent was removed by evaporation, and to the resultant mixture was added CH_2Cl_2 (75 mL). The mixture was washed with water (50 mL × 3), 10% NH_4Cl (60 mL × 3), and sat. brine (50 mL), and then dried over anhydrous $MgSO_4$, followed by removal of the solvent. Purification of the residue by silica gel column chromatography (40:1 CH_2Cl_2−MeOH, v/v, as eluent) followed by recrystallization from CH_2Cl_2−hexane yielded a dark blue crystal of **16c** (134 mg, 0.210 mmol, 42%): mp 238−241 °C (dec); ^{1}H NMR (500 MHz, $CDCl_3$) δ 1.24 (t, J = 7.3 Hz, 6H), 1.61 (t, J = 7.6 Hz, 6H), 1.67 (t, J = 7.6 Hz, 6H), 2.15 (sextet, J = 7.3 Hz, 4H), 3.06 (s, 6H), 3.33−3.39 (m, 2H), 3.41−3.47 (m, 2H), 3.48−3.60 (m, 8H), 9.21 (s, 2H), 9.27 (s, 1H); IR (KBr) 2962, 2931, 2869, 1549, 1204 cm^{-1}; FAB MS m/z 599 ([M − Cl]$^+$); HR FAB MS calcd for $[C_{35}H_{43}N_4O^{64}Zn]^+$ 599.2728, found 599.2701. Anal. Calcd for $C_{35}H_{43}N_4OClZn$: C, 66.04; H, 6.81; N, 8.80. Found: C, 66.41; H, 6.96; N, 8.79.

3,8,12,17-Tetraethyl-1,21-dihydro-19-methoxy-2,7,13,18-tetramethyl-22*H*-bilin-1-one (17a). A mixture of **16a** (250 mg, 0.431 mmol) and sodium methoxide (73 mg, 1.35 mmol) in dry MeOH (55 mL) was stirred at room temperature for 1.5 h. To the reaction mixture was added 10% NH_4Cl (100 mL), followed by extractive work up with $CHCl_3$ (55 mL × 2). The organic layer was washed with 10% NH_4Cl (100 mL × 2) and vigorously shaken with phthalate buffer (pH = 4.01, 100 mL × 2). The dark green solution then turned blue. The solution was washed with water (100 mL) and sat. brine (100 mL). After the extracts were dried over anhydrous Na_2SO_4, the solvent was removed by evaporation. Purification of the residue by silica gel column chromatography (75:1 CH_2Cl_2−MeOH, v/v, as eluent) followed by recrystallization from $CHCl_3$−hexane yielded **17a** as a dark blue solid (181 mg, 0.354 mmol, 82%): mp 229−231 °C (dec), (lit.[31] mp 233−235 °C); ^{1}H NMR (500 MHz, $CDCl_3$) δ 1.13−1.18 (m, 9H), 1.19 (t, J = 7.9 Hz, 3H), 1.73 (s, 3H), 1.84 (s, 3H), 2.02 (s, 3H), 2.11 (s, 3H), 2.47 (q, J = 7.9 Hz, 4H), 2.54 (q, J = 7.9 Hz, 2H), 2.57 (q, J = 7.9 Hz, 2H), 3.97 (s, 3H), 5.76 (s, 1H), 6.29 (s, 1H), 6.61 (s, 1H), 10.2 (br s, 1H), 12.9 (br s, 1H); IR (KBr) 3445, 2961, 2925, 2865, 1701, 1627, 1588, 1212 cm^{-1}; EI MS (rel intensity) m/z 512 (M$^+$, 100), 497 (74), 483 (30). Anal. Calcd for $C_{32}H_{40}N_4O_2$: C, 74.97; H, 7.86; N, 10.93. Found: C, 74.57; H, 8.00; N, 10.88.

3,7-Bis(2-acetoxyethyl)-3,8,12,17-tetraethyl-1,21-dihydro-19-methoxy-7,13-dimethyl-22*H*-bilin-1-one (17b). A mixture of **16b** (204 mg, 0.282 mmol) and sodium methoxide (17.9 mg, 0.331 mmol) in dry MeOH (17 mL) was stirred at room temperature for 4 h. Dichloromethane (60 mL) was added, and the mixture was washed with water (60 mL) and then vigorously shaken with phthalate buffer (pH = 4.01, 60 mL × 3). The organic layer was washed with sat. brine (60 mL) and dried over anhydrous Na_2SO_4, followed by removal of the solvent. Purification of the residue by silica gel column chromatography (100:1 CH_2Cl_2−MeOH, v/v, as eluent) followed by recrystallization from CH_2Cl_2−hexane yielded a dark blue crystal of **17b** (132 mg, 0.201 mmol, 71%): mp 146−148 °C (dec); ^{1}H NMR (500 MHz, $CDCl_3$) δ 1.13−1.16 (m, 6H), 1.20 (t, J = 7.9 Hz, 3H) 1.22 (t, J = 7.6 Hz, 3H), 2.01 (s, 3H), 2.020 (s, 3H), 2.022 (s, 3H), 2.10 (s, 3H), 2.47−2.59 (m, 10H), 2.63 (t, J = 7.0 Hz, 2H), 4.02 (s, 3H), 4.06 (t, J = 7.0 Hz, 2H), 4.14 (t, J = 7.0 Hz, 2H), 5.78 (s, 1H), 6.31 (s, 1H), 6.59 (s, 1H), 10.42 (br s, 1H), 13.04 (br s, 1H); IR (KBr) 3444, 2967, 2933, 2871, 1739, 1697, 1590, 1242, 1213 cm^{-1}; FAB MS m/z 657 (M + H$^+$); HR FAB MS calcd for $[C_{38}H_{48}N_4O_6]^+$ 656.3574, found 656.3553. Anal. Calcd for $C_{38}H_{48}N_4O_6$: C, 69.49; H, 7.37; N, 8.53. Found: C, 69.29; H, 7.57; N, 8.06.

3,8,12,17-Tetraethyl-1,21-dihydro-3,7-bis(2-hydroxyethyl)-19-methoxy-7,13-dimethyl-22*H*-bilin-1-one (17c). A mixture of **16b** (126 mg, 0.218 mmol) and sodium methoxide (126 mg, 2.33 mmol) in dry MeOH (13 mL) was stirred at room temperature for 4 h. Dichloromethane (50 mL) was added, and the mixture was washed with water (50 mL) and then vigorously shaken with phthalate buffer (pH = 4.01, 50 mL × 3). The solution was washed with sat. brine (50 mL) and dried over anhydrous Na_2SO_4, followed by removal of the solvent. Purification of the residue by silica gel column chromatography (30:1 CH_2Cl_2−MeOH, v/v, as eluent) followed by recrystallization from CH_2Cl_2−hexane yielded a dark blue crystal of **17c** (96.0 mg, 0.168 mmol, 77%): mp 171−173 °C (dec); ^{1}H NMR (500 MHz, $CDCl_3$) δ 1.12−1.15 (m, 6H), 1.19 (t, J = 7.3 Hz, 3H), 1.22 (t, J = 7.3 Hz, 3H), 2.00 (s, 3H), 2.08 (s, 3H), 2.40−2.57 (m, 12H), 3.16 (br s, 1H, D_2O exchangeable), 3.65 (br s, 1H, D_2O exchangeable), 3.67−3.69 (m, 4H), 4.15 (s, 3H), 5.77 (s, 1H), 6.26 (s, 1H), 6.55 (s, 1H), 10.88 (br s, 1H), 13.43 (br s, 1H); IR (KBr) 3343, 2965, 2931, 2872, 1680, 1587, 1218 cm^{-1}; FAB MS m/z 572 (M + H$^+$); HR FAB MS calcd for $[C_{34}H_{44}N_4O_4]^+$ 572.3363, found 572.3375. Anal. Calcd for $C_{34}H_{44}N_4O_4$: C, 71.30; H, 7.74; N, 9.78. Found: C, 70.91; H, 7.89; N, 9.68.

3,8,12,17-Tetraethyl-1,21-dihydro-2,7,13,18-tetramethyl-19-(2-propoxy)-22*H*-bilin-1-one (17d). This compound was prepared by a procedure similar to **17b** using **16a** (174 mg, 0.300 mmol) and sodium 2-propoxide (3 mL, 0.3 M in 2-propanol) and 2-propanol (30 mL). After the reaction was completed, the mixture was treated with 10% NH_4Cl (40 mL), followed by extractive work up with $CHCl_3$ (40 mL × 3). The organic layer was washed with 10% NH_4Cl (40 mL × 3) and vigorously shaken with phthalate buffer (pH = 4.01, 40 mL × 3). The solution was washed with water (50 mL × 2) and sat. brine (50 mL). After drying the extracts were dried anhydrous Na_2SO_4, the solvent was removed by evaporation. Purification of the resultant mixture by silica gel column chromatography

(31) Falk, H.; Grubmeyer, K.; Thirring, K. *Z. Naturforsh.* **1978**, *33b*, 924−931.

(100:1 CH_2Cl_2−MeOH, v/v, as eluent) followed by recrystallization from $CHCl_3$−hexane yielded **17d** as a dark blue crystal (133 mg, 0.245 mmol, 82%): mp 199−201 °C (dec); ^{1}H NMR (500 MHz, $CDCl_3$) δ 1.13−1.19 (m, 18H), 1.74 (s, 3H), 1.84 (s, 3H), 2.04 (s, 3H), 2.12 (s, 3H), 2.44−2.50 (m, 4H), 2.52−2.61 (m, 4H), 5.31 (spt, J = 6.1 Hz, 1H), 5.81 (s, 1H), 6.28 (s, 1H), 6.64 (s, 1H), 10.17 (br s, 1H), 12.65 (br s, 1H); IR (KBr) 3461, 2961, 2930, 2867, 1701, 1582, 1209 cm^{-1}; FAB MS m/z 540 ([M$^+$]); HR FAB MS calcd for $[C_{34}H_{44}N_4O_2]^+$ 540.3464, found 540.3483. Anal. Calcd for $C_{34}H_{44}N_4O_2$: C, 75.52; H, 8.20; N, 10.40. Found: C, 75.82; H, 8.18; N, 10.27.

3,8,12,17-Tetraethyl-1,21-dihydro-19-methoxy-7,13-dimethyl-2,18-dipropyl-22*H*-bilin-1-one (17e). A mixture of **16c** (127 mg, 0.200 mmol) and sodium methoxide (33.0 mg, 0.61 mmol) in dry MeOH (20 mL) was stirred at room temperature for 1 h. To the reaction mixture was added $CHCl_3$ (30 mL), followed by washing with 10% NH_4Cl (30 mL). The organic layer was vigorously shaken with phthalate buffer (pH = 4.01, 30 mL × 3), and the dark green solution then turned blue. The organic layer was washed with water (30 mL) and sat. brine (30 mL). After drying the extracts over anhydrous Na_2SO_4, the solvent was removed by evaporation. Purification of the residue by silica gel column chromatography (75:1 CH_2Cl_2−MeOH, v/v, as eluent) followed by recrystallization from CH_2Cl_2−hexane yielded **17e** as a dark blue crystal (85.2 mg, 0.150 mmol, 75%): mp 215−217 °C (dec); ^{1}H NMR (270 MHz, $CDCl_3$) δ 0.86−0.94 (m, 6H), 1.11−1.26 (m, 12H), 1.36−1.54 (m, 4H), 2.01 (s, 3H), 2.10 (s, 3H), 2.12−2.17 (m, 2H), 2.24 (t, J = 7.3 Hz, 2H), 2.43−2.61 (m, 8H), 3.99 (s, 3H), 5.75 (s, 1H), 6.28 (s, 1H), 6.60 (s, 1H), 10.3 (br s, 1H), 12.9 (br s, 1H); IR (KBr) 2961, 2930, 2868, 1701, 1582, 1209 cm^{-1}; FAB MS m/z 568 ([M$^+$]); HR FAB MS calcd for $[C_{36}H_{48}N_4O_2]^+$ 568.3777, found 568.3758. Anal. Calcd for $C_{36}H_{48}N_4O_2$: C, 76.02; H, 8.51; N, 9.85. Found: C, 75.97; H, 8.65; N, 9.63.

Preparation of Amino Alcohol Methyl Ethers. Preparation of amino alcohol methyl ethers followed the literature procedure.[32] The optical purity of each compound was checked by ^{1}H NMR of their (+)-benzylmethylphenylsilylacetylamide derivatives.[33] For example, the $SiCH_3$ signals of the amide derived from racemic **24** appeared at 0.35 and 0.37 ppm. There was no peak at 0.35 ppm in the ^{1}H NMR spectra of (*S*)-**24** prepared here, showing that its enantiomeric excess is higher than 90%. A similar result was obtained for **23**.

(*S*)-2-Amino-1-methoxy-3-phenylpropane (Phenylalaninol Methyl Ether, 23). Potassium hydride (2.95 g, 0.0257 mol, 35 wt % oil dispersion) was placed in a flask and washed with hexane several times. THF (50 mL) was added, and to the suspension was added dropwise (*S*)-2-amino-1-hydroxy-3-phenylpropane (4.09 g, 0.027 mol) dissolved in THF (50 mL). The mixture was stirred overnight at room temperature and then cooled to 0 °C. Iodomethane (3.57 g, 0.0252 mol) in THF (10 mL) was added dropwise over 30 min. After 1 h of stirring, the mixture was poured into ice (10 g), followed by addition of 100 mL of water. The THF was removed by evaporation, and the aqueous mixture was extracted with hexane (50 mL × 3). The organic phase was dried over anhydrous $MgSO_4$, and the solvent was then removed on a rotary evaporator. Distillation at the reduced pressure (4 mmHg) yielded pure (*S*)-**23** as a colorless oil (2.45 g, 0.0148 mol, 55%): bp 100−102 °C at 4 mmHg (lit.[32] 95−100 °C at 15 mmHg); ^{1}H NMR (500 MHz, $CDCl_3$) δ 1.43 (br s, 2H), 2.55 (dd, J = 13.4, 7.9 Hz, 1H), 2.78 (dd, J = 13.4, 4.9 Hz, 1H), 3.21−3.24 (m, 2H), 3.35−3.39 (m, 4H), 7.20−7.23 (m, 3H), 7.29−7.32 (m, 2H); ^{13}C NMR (125 MHz, $CDCl_3$) δ 40.8, 52.3, 58.9, 77.4, 126.3, 128.4, 129.2, 138.8.

(+)-Benzylmethylphenylsilylacetamide Derived from (*S*)-2-Amino-1-methoxy-3-phenylpropane. Conversion to the amide was carried out according to the procedure of Nohira.[33] A mixture of (*S*)-**23** (19.2 mg, 0.116 mmol), (+)-benzylmethylphenylsilylacetic acid (31.5 mg, 0.116 mmol), 2-chloro-1-methylpyridinium iodide (34.5 mg, 0.135 mmol), and tributylamine (53.7 mg, 0.290 mmol) in 1 mL of dry CH_2Cl_2 was stirred at reflux under argon for 1.5 h. Purification by silica gel thin-layer chromatography (hexane−ethyl acetate 1:1 (v/v) as eluent) yielded the amide of (+)-benzylmethylphenylsilylacetic acid with (*S*)-**23** (36.9 mg, 0.0884 mmol, 76%): ^{1}H NMR (270 MHz, $CDCl_3$) δ 0.31 (s, 3H), 1.94 (d, J = 12.8 Hz, 1H), 2.00 (d, J = 12.8 Hz, 1H), 2.43 (d, J = 14.0 Hz, 1H), 2.50 (d, J = 14.0 Hz, 1H), 2.59−2.72 (m, 2H), 3.06 (dd, J = 9.5, 3.7 Hz, 1H), 3.16 (dd, J = 9.5, 3.7 Hz, 1H), 3.25 (s, 3H), 4.10−4.23 (m, 1H), 5.32 (d, J = 8.6 Hz, 1H), 6.99 (dd, J = 7.6, 1.8 Hz, 2H), 7.04−7.42 (m, 11H), 7.46 (dd, J = 7.6, 1.8 Hz, 2H); FAB MS m/z 418 ([M + H]$^+$).

The ^{1}H NMR spectrum of the amide showed that the enantiomeric excess of the amine is higher than 90%; the $SiCH_3$ signal in the ^{1}H NMR spectrum was observed only at 0.31 ppm, while that of the amide derived from (+)-benzylmethylphenylsilylacetic acid and racemic 2-amino-1-methoxy-3-phenylpropane was observed at 0.31 and 0.33 ppm.

(*S*)-2-Amino-1-methoxy-4-methylpentane (Leucinol Methyl Ether, 24). The synthesis of (*S*)-**24** was carried out similarly. Potassium hydride (3.93 g, 0.0343 mol, 35 wt % oil dispersion) was placed in a flask and washed with hexane several times. THF (45 mL) was added, and to the suspension was then added dropwise (*S*)-2-amino-1-hydroxy-4-methylpentane (4.02 g, 0.0343 mol) dissolved in THF (30 mL). The mixture was stirred overnight at room temperature and then cooled to 0 °C. Iodomethane (4.87 g, 0.0343 mol) in THF (45 mL) was added dropwise over 30 min. After 30 min of stirring, the mixture was poured into ice (15 g), followed by addition of 30 mL of water. The THF was removed by evaporation, and the aqueous mixture was extracted with hexane (30 mL × 3). The organic phase was dried over anhydrous $MgSO_4$, and the solvent was then removed on a rotary evaporator. Distillation at the reduced pressure yielded pure (*S*)-**24** as a colorless oil (1.21 g, 0.00922 mol, 27%): bp 63.5−64.5 °C at 25 mmHg; ^{1}H NMR (500 MHz, $CDCl_3$) δ 0.90 (d, J = 6.7 Hz, 3H), 0.93 (d, J = 6.7 Hz, 3H), 1.16−1.20 (m, 2H), 1.43 (br s, 2H), 1.69−1.78 (m, 1H), 3.00−3.05 (m, 1H), 3.11 (dd, J = 8.9, 7.9 Hz, 1H), 3.33 (dd, J = 8.9, 3.7 Hz, 1H), 3.36 (s, 3H); ^{13}C NMR (125 MHz, $CDCl_3$) δ 22.0, 23.4, 24.6, 43.3, 48.6, 58.9, 78.8.

(+)-Benzylmethylphenylsilylacetamide Derived from (*S*)-2-Amino-1-methoxy-4-methylpentane. A mixture of (*S*)-**24** (14.2 mg, 0.108 mmol), (+)-benzylmethylphenylsilylacetic acid (29.2 mg, 0.108 mmol), 2-chloro-1-methylpyridinium iodide (33.1 mg, 0.130 mmol), and tributylamine (50.0 mg, 0.270 mmol) in 1 mL of dry CH_2Cl_2 was stirred at reflux under argon for 1.5 h. Purification by silica gel thin-layer chromatography (hexane−ethyl acetate 1:1 (v/v) as eluent) yielded the amide of (+)-benzylmethylphenylsilylacetic acid with (*S*)-**24** (36.0 mg, 0.0938 mmol, 87%): ^{1}H NMR (270 MHz, $CDCl_3$) δ 0.37 (s, 3H), 1.16 (t, J = 7.3 Hz, 1H), 1.96 (d, J = 12.8 Hz, 1H), 2.01 (d, J = 12.8 Hz, 1H), 2.43 (d, J = 14.0 Hz, 1H), 2.50 (d, J = 14.0 Hz, 1H), 3.17 (dd, J = 9.5, 3.7 Hz, 1H), 3.22 (dd, J = 9.5, 3.7 Hz, 1H), 3.25 (s, 3H), 4.09−3.97 (m, 1H), 5.05 (d, J = 8.6 Hz, 1H), 6.99 (dd, J = 7.6, 1.8 Hz, 2H), 7.14−7.04 (m, 1H), 7.26−7.15 (m, 2H), 7.42−7.31 (m, 3H), 7.47 (dd, J = 7.6, 1.8 Hz, 2H); FAB MS m/z 384 ([M + H]$^+$).

1-Naphthylmethyl *N*-*tert*-Butoxycarbonyl-L-leucinate. To a stirred mixture of *N*-Boc-leucine monohydrate (997 mg, 4.00 mmol), 1-naphthylmethanol (633 mg, 4.00 mmol), and 4-(*N*,*N*-dimethylamino)pyridine (54 mg, 0.44 mmol) in dry CH_2Cl_2 (15 mL) was added 1-ethyl-3-(3-dimethylaminopropyl)-carbodiimide hydrochloride (843 mg, 4.40 mmol) at 0 °C. The mixture was stirred at the same temperature and then stirred overnight at ambient temperature. The solvent was removed by evaporation, and the residue was dissolved in ethyl acetate (150 mL). The solution was washed with sat. Na_2CO_3 (30 mL × 2), water (30 mL × 2), and saturated brine (30 mL) and dried over anhydrous $MgSO_4$. Purification by silica gel column chromatography afforded *N*-*tert*-butoxycarbonyl-L-leucine 1-naphthylmethyl ester as a syrup (977 mg, 2.63 mmol, 66%): ^{1}H NMR (500 MHz, $CDCl_3$) δ 0.85 (d, J = 6.1 Hz, 3H), 0.86 (d, J = 6.1 Hz, 3H), 1.40−1.71 (m, 12H), 4.34−4.39 (m, 1H), 4.91 (d, J = 8.6 Hz, 1H), 5.59 (d, J = 12.5 Hz, 1H), 5.65 (d, J = 12.5 Hz, 1H), 7.45 (t, J = 7.9 Hz, 1H), 7.49−7.57 (m, 3H), 7.85

(32) Welch, J. T.; Seper, K. W. *J. Org. Chem.* **1988**, *53*, 2991−2999.
(33) Terunuma, D.; Kato, M.; Kamei, M.; Uchida, H.; Ueno, S.; Nohira, H. *Bull. Chem. Soc. Jpn.* **1986**, *59*, 3581−3587.

(d, 1H, J = 7.9 Hz), 7.88 (d, 1H, J = 8.6 Hz), 7.99 (d, 1H, J = 8.6 Hz); ^{13}C NMR (125 MHz, $CDCl_3$) δ 21.8, 22.7, 24.7, 28.3, 41.6, 52.3, 65.2, 79.8, 123.5, 125.2, 125.9, 126.6, 127.5, 128.7, 129.4, 130.7, 131.5, 133.7, 155.35, 173.3; IR (CCl_4) 3441, 2960, 2932, 2873, 1743, 1721 cm^{-1}; FAB MS m/z 372 ([M + H]$^+$).

1-Naphthylmethyl L-leucinate (L-Leu-ONp). To 20 mL of trifluoroacetic acid (TFA) was added 1-naphthylmethyl *N*-*tert*-butoxycarbonyl-L-leucinate (1.62 g, 4.36 mmol), and the mixture was stirred for 30 min at room temperature. After removal of the TFA at the reduced pressure by water aspirator, the residue was dissolved in CH_2Cl_2 (25 mL), followed by washing with saturated $NaHCO_3$ (25 mL×3), water (25 mL), and sat. brine (25 mL). The solution was dried over anhydrous $MgSO_4$, and the solvent was removed by evaporation. Purification by silica gel column chromatography using CH_2Cl_2 as eluant afforded 1-naphthylmethyl L-leucinate as an oil (415 mg, 1.53 mmol, 35%): ^{1}H NMR (500 MHz, $CDCl_3$) δ 0.86 (d, J = 6.7 Hz, 3H), 0.88 (d, J = 6.7 Hz, 3H), 1.42 (ddd, J = 13.6, 8.2, and 6.1 Hz, 1H), 1.56 (ddd, J = 13.6, 8.2, and 5.8 Hz, 1H), 1.57 (br s, 2H), 1.67−1.78 (m, 1H), 3.51 (dd, J = 8.2, 5.8 Hz, 1H), 5.59 (d, J = 12.5 Hz, 1H), 5.62 (d, J = 12.5 Hz, 1H), 7.44−7.47 (m, 1H), 7.51−7.57 (m, 3H), 7.86 (d, J = 8.2 Hz, 1H), 7.88 (dd, J = 8.2, 1.5 Hz, 1H), 8.00 (d, J = 8.2 Hz, 1H); ^{13}C NMR (125 MHz, $CDCl_3$) δ 21.8, 22.9, 24.7, 44.0, 53.0, 64.9, 123.5, 125.2, 126.0, 126.5, 127.6, 128.7, 129.4, 131.2, 131.6, 133.7, 176.5; IR (CCl_4) 3443, 2959, 2932, 2872, 1736 cm^{-1}; FAB MS m/z 272 ([M + H]$^+$); $[\alpha]^{23}_D$ +4.9° (c 0.53, CH_2Cl_2).

Analysis of Binding Constants by ^{1}H NMR Spectroscopy. The binding constants of **4**−**8** with amino acid esters and amines, K_{223} and K_{223}', were obtained by least-squares curve fitting of ^{1}H NMR complexation-induced shifts to the theoretical equations. In the present case, the following equations are taken into consideration:

$$K_{223} = [M{-}G]/[M]\cdot[G] \quad (1)$$

$$K_{223}' = [P{-}G]/[P]\cdot[G] \quad (2)$$

$$[P] = [M] \quad (3)$$

$$[H]_0 = [M] + [P] + [M{-}G] + [P{-}G] \quad (4)$$

$$[G]_0 = [G] + [M{-}G] + [P{-}G] \quad (5)$$

where [M], [P], [G], [M−G], and [P−G] are the concentrations of M-host, P-host, guest, the M-host·guest complex, and the P-host·guest complex, respectively, and $[H]_0$ and $[G]_0$ are the total concentrations of the host and the guest, respectively.

Since the helix inversion of ZnBD is slow and the complex formation and dissociation are fast on the NMR time scale at lower temperatures, the following equations gave the observed chemical shifts, δ_{obs} and δ_{obs}', for M species and P species, respectively:

$$\delta_{obs} = \{[M{-}G]/([M] + [M{-}G])\}\cdot\delta_{M-G} + \{[M]/([M] + [M{-}G])\}\cdot\delta_M \quad (6)$$

$$\delta_{obs}' = \{[P{-}G]/([P] + [P{-}G])\}\cdot\delta_{P-G} + \{[P]/([P] + [P{-}G])\}\cdot\delta_P \quad (7)$$

where the δ_M, δ_P, δ_{M-G}, and δ_{P-G} are the chemical shifts of the protons of M-host, P-host, the M-host·guest complex, and the P-host·guest complex, respectively. In the present case, δ_M and δ_P are the same, and δ_{M-G} and δ_{P-G} are obtained by extrapolation of the titration curves.

If $[H]_0$ and $[G]_0$ are given, [M], [P], [M−G], and [P−G] are derived from eqs 1−5 as functions of K_{223} and K_{223}'. Therefore, δ_{obs} and δ_{obs}' are also represented as functions of K_{223} and K_{223}'. The ^{1}H NMR measurements in the presence of varying concentrations of the guest afford the titration curves of the chemical shift changes, which are fitted to the theoretical eqs 6 and 7 by optimizing K_{223} and K_{223}'. The numerical calculations were carried out with computer assistance based on a damping Gauss−Newton method, finally, to give K_{223} and K_{223}'.

Acknowledgment. This work was supported by a Grant-in Aid for Scientific Research from the Ministry of Education, Science, Sports, and Culture, Japan. We appreciate Professor Toshikazu Takata's kind cooperation in the measurements of optical rotation. We thank T. Kobatake for help in mass spectroscopic studies. We also thank Professor Hiroyuki Nakazumi for his kind help in IR studies.

Supporting Information Available: ^{1}H−^{1}H NOESY spectrum of compound **4**, and ^{1}H NMR spectrum of compound **13c** (2 pages). This material is contained in libraries on microfiche, immediately follows this article in the microfilm version of the journal, and can be ordered from the ACS; see any current masthead page for ordering information.

JO980819J